

Nucleus - Air Interactions for Extensive Air Showers Experiments at Ultrahigh Energies*

V.Topor Pop

Physics Department, Columbia University, New York, NY 10027

and

Dipartimento di Fisica "G.Galilei"; Istituto di Fisica Nucleare

Sezione di Padova,

Via Marzolo 8-35131, Padova, Italy

and

H.Rebel

Kernforschungszentrum Karlsruhe, Institut für Kernphysik III,

P.O.Box 3640, D-76021 Karlsruhe, Germany

October 17, 2018

Work to be submitted to Astroparticle Physics

*This work was supported by the Director, Office of Energy Research, Division of Nuclear Physics of the Office of High Energy and Nuclear Physics of the U.S. Department of Energy under Contract No. DE-AC03-76SF00098

E-mail TOPOR@PADOVA.INFN.IT ; TOPOR@ROIFA.BITNET

TOPOR@NT1.PHYS.COLUMBIA.EDU

Abstract

The HIJING and VENUS models of relativistic hadron-nucleus and nucleus-nucleus collisions are used to study interactions of proton and nuclei with nitrogen, specific for the extensive air shower developments initiated by cosmic rays in the atmosphere. The transverse energy, transverse momenta and secondary particles produced spectra as well as their energy and mass dependence were investigated in detail. Results are presented with particular emphasis on the contributions of minijets in HIJING model and validity of superposition models in this energy range .

PACS : 13.85.Hd ; 13.85.Ni ; 13.85.Tp ; 96.40.De;96.40.Pq;96.40.Tv

1 Introduction

The investigation of the detailed shape of the energy spectrum and the mass composition of primary cosmic rays is currently a most active field of astrophysical research [1].

Experiments on satellites or with balloon-borne detectors give information up to energies of ca. 10^{14} eV [2]. Due to their limitations in size and weight they can hardly be extended beyond 10^{15} eV, and indirect techniques, the observation of the particle-cascades in the atmosphere (extensive air showers: EAS), have to be invoked. The information about nature and energy of the primary particles is reflected by the shower development [3] whose details and signatures for the primary particle depend on the high-energy nuclear interactions, governing the cascading processes. Thus the analysis requires a reliable description of these processes, formulated as a hadronic interaction model which can be used as generator of Monte-Carlo simulations of air showers. It should describe the currently available experimental information from accelerator experiments (in particular the data from the large collider facilities at CERN and Fermilab) and allow a justified extrapolation to experimentally unexplored energy regions. In the case of the EAS cascades, the quest is for the cross sections (multi-particle production, rapidity and transverse momentum distributions) for hadron-hadron, hadron-nucleus and nucleus-nucleus collisions as function of the energy (from pion production threshold up to ultrahigh energies), most importantly for the forward fragmentation region, while actually the central region of the collisions is best studied at accelerators. The fragmentation region is nevertheless also relevant for the interaction models describing the experimental observations at SPS energies and beyond [4],[5],[6].

There are many hadronic transport models en vogue which address this problem. They comprise versions of the Dual-Parton model (DPM) [7], Quark-Gluon String models (QGSM) [8], and models designated with the name of the code like VENUS [9], FRITIOF [10], HIJING [11]-[14], Parton Cascade Models [15],[16] and others. Some have been specifically developed as Monte-Carlo generator for air shower simulations at cosmic ray energies like DPM [17], HEMAS [18] and SYBILL [19].

Recently [20] the VENUS approach, linked to the CORSIKA code [21] (now widely used for cosmic rays EAS simulations) has been used to scrutinize the superposition hypothesis in nucleus-nucleus collisions at ultrahigh energies. The hypothesis has been shown to be a rather good approximation, for the air shower cascade while Ranft [6] using the DPMJET-II version of the DPM approach and considering the fragmentation and central regions with equal importance concluded that the superposition is a rather rough approximation of the reality. Our present work is based on the experience with a model and its extensions which are the basis of the HIJING code and used for an extrapolation of the particle production

dynamics from proton-proton (pp) to proton-nucleus (pA) and nucleus-nucleus (AA) interactions, taking into account the essential constraints of geometry and kinematics. At higher collision energies semi-hard processes are included by perturbative QCD processes (pQCD).

While the HIJING model ignores final state interactions, the VENUS model includes reinteractions of string segments among themselves and with spectator matter, with occurrence of "double strings" which mediate multinucleon interactions in nucleus-nucleus collisions.

Both string-models have been applied to a variety of pp, pA and AA collision data (see references [9],[12],[13], [22]). However, a consistent intercomparison of predictions of multiparticle production, transverse momentum and rapidity distributions at ultrahigh energies and with respect to their relevance in the EAS cascade is missing. The present paper is a first attempt of such a comparison, revealing the most salient features and differences in a selected number of cases. We introduce the presentation of numerical results with a brief reminder of the basis of the HIJING model under consideration, stressing the different procedures in defining the interacting nucleon configurations, the quark-gluon string formation and the decay into secondary particles.

The models have been tested at accelerator energies for proton-proton and nucleus-nucleus interactions and then theoretical predictions on pseudorapidity distributions of transverse energy, transverse momenta and secondary particles spectra as well as their energy and mass dependence are given using HIJING model for proton - Air Nucleus (p+Air) interactions between 1 TeV - 1000 TeV and for Nucleus - Air (A+Air) interactions at 17.86 TeV/Nucleon corresponding to 1 PeV for iron (Fe) nucleus. A comparison with recent results [20] at the same energy using VENUS model is also done. We have investigated Feynman scaling behaviour of the model in this energy region, and the multiple minijets production is considered for study of the charged multiplicity distributions. Finally a brief discussion on validity of superposition models, taken into consideration mean integrated values of transverse energy predicted by HIJING model, is presented.

2 Outline of HIJING Model

A detailed discussion of the HIJING Monte Carlo model was reported in references [11]-[14]. The formulation of HIJING was guided by the LUND-FRITIOF and Dual Parton Model(DPM) phenomenology for soft nucleus-nucleus reactions at intermediate energies ($\sqrt{s} < 20 \text{ GeV}$) and implementation pQCD processes in the PHYTHIA model[23] for hadronic interactions. We give in this section a brief review of the aspect of the model relevant to hadronic interaction:

1. Exact diffuse nuclear geometry is used to calculate the impact parameter dependence of the number of inelastic processes.
2. Soft beam jets are modeled by quark-diquark strings with gluon kinks along the lines of the DPM and FRITIOF models. Multiple low p_T exchanges among the end point constituents are included.
3. The model includes multiple mini-jet production with initial and final state radiation along the lines of the PYTHIA model and with cross sections calculated within the eikonal formalism.
4. The hadronization of single chains is handled by the LUND code JETSET 7.3 [23], that summarizes data on e^+e^- . In this picture, each nucleon-nucleon collision results in excitation of the nucleon by the stretching of a string between the valence quark and diquark (longitudinal excitation, without colour exchange). A phenomenological excitation function determines the mass and momentum of the string after each interaction. After the last interaction the string decays to produce particles.
5. HIJING does not incorporate any mechanism for final state interactions among low p_T produced particles nor does it have colour rope formation.

Unlike heavy ion collisions at the existing AGS/BNL and SPS/CERN energies, most of the physical processes occurring at very early times in the violent collisions of heavy nuclei at cosmic ray energies involve hard or semihard parton scatterings which will result in enormous amount of jet production and can be described in terms of pQCD. Assuming independent production, it has been shown that the multiple minijets production is important in proton-antiproton ($p\bar{p}$) interactions to account for the increase of total cross section [24] and the violation of Koba-Nielsen-Olesen (KNO) scaling of the charged multiplicity distributions [12].

In high energy heavy ion collisions, minijets have been estimated [25] to produce 50% (80%) of the transverse energy in central heavy ion collisions at RHIC (LHC) energies. While not resolvable as distinct jets, they would lead to a wide variety of correlations, as in proton-proton (pp) or antiproton-proton $\bar{p}p$ collisions, among observables such as multiplicity, transverse momentum, strangeness, and fluctuations that compete with the expected signatures of a QGP. Therefore, it is especially important to calculate these background processes.

These processes are calculated in pQCD starting with the cross section of hard parton scatterings [26] :

$$\frac{d\sigma_{jet}}{dP_T^2 dy_1 dy_2} = K \sum_{a,b} x_1 x_2 f_a(x_1, P_T^2) f_b(x_2, P_T^2) d\sigma^{ab}(\hat{s}, \hat{t}, \hat{u})/d\hat{t}, \quad (1)$$

where the summation runs over all parton species, y_1, y_2 are the rapidities of the scattered partons and x_1, x_2 are the fractions of momentum carried by the initial partons and they are related by $x_1 = x_T(e^{y_1} + e^{y_2})/2$, $x_2 = x_T(e^{-y_1} + e^{-y_2})$, $x_T = 2P_T/\sqrt{s}$. A factor, $K \approx 2$ accounts roughly for the higher order corrections. The default structure functions, $f_a(x, Q^2)$, in HIJING are taken to be Duke-Owens structure function set 1 [27].

Integrating Eq. 1 with a low P_T cutoff P_0 , one obtain the total inclusive jet cross section σ_{jet} . The average number of semihard parton collisions for a nucleon-nucleon collision at impact parameter b is $\sigma_{jet}T_N(b)$, where $T_N(b)$ is partonic overlap function between the two nucleons. In terms of a semiclassical probabilistic model [24, 12], the probability for multiple minijets production is :

$$g_j(b) = \frac{[\sigma_{jet}T_N(b)]^j}{j!} e^{-\sigma_{jet}T_N(b)}, \quad j \geq 1. \quad (2)$$

Similarly, the soft interactions are represented by an inclusive cross section σ_{soft} which, unlike σ_{jet} , can only be determined phenomenologically. The probability for only soft interactions without any hard processes is :

$$g_0(b) = [1 - e^{-\sigma_{soft}T_N(b)}] e^{-\sigma_{jet}T_N(b)}. \quad (3)$$

and the total inelastic cross section for nucleon-nucleon collisions :

$$\begin{aligned} \sigma_{in} &= \int d^2b \sum_{j=0}^{\infty} g_j(b) \\ &= \int d^2b [1 - e^{-(\sigma_{soft} + \sigma_{jet})T_N(b)}]. \end{aligned} \quad (4)$$

Define a real eikonal function,

$$\chi(b, s) \equiv \frac{1}{2}\sigma_{soft}(s)T_N(b, s) + \frac{1}{2}\sigma_{jet}(s)T_N(b, s), \quad (5)$$

the elastic, inelastic, and total cross sections of nucleon-nucleon collisions are given by :

$$\sigma_{el} = \pi \int_0^\infty db^2 \left[1 - e^{-\chi(b,s)}\right]^2, \quad (6)$$

$$\sigma_{in} = \pi \int_0^\infty db^2 \left[1 - e^{-2\chi(b,s)}\right], \quad (7)$$

$$\sigma_{tot} = 2\pi \int_0^\infty db^2 \left[1 - e^{-\chi(b,s)}\right], \quad (8)$$

Assuming that the parton density in a nucleon can be approximated by the Fourier transform of a dipole form factor, the overlap function is :

$$T_N(b, s) = 2 \frac{\chi_0(\xi)}{\sigma_{soft}(s)}, \quad (9)$$

with

$$\chi_0(\xi) = \frac{\mu_0^2}{96}(\mu_0\xi)^3 K_3(\mu_0\xi), \quad \xi = b/b_0(s), \quad (10)$$

where $\mu_0 = 3.9$ and $\pi b_0^2(s) \equiv \sigma_0 = \sigma_{soft}(s)/2$ is a measure of the geometrical size of the nucleon. The eikonal function can be written as :

$$\chi(b, s) \equiv \chi(\xi, s) = [1 + \sigma_{jet}(s)/\sigma_{soft}(s)]\chi_0(\xi). \quad (11)$$

$P_0 \simeq 2$ GeV/ c and a constant value of $\sigma_{soft}(s) = 57$ mb are chosen to fit the experimental data on cross sections [12] in pp and $p\bar{p}$ collisions. The equations listed above are used to simulate multiple jets production at the level of nucleon-nucleon collisions in HIJING Monte Carlo program. Once the number of hard scatterings is determined, PYTHIA algorithms generate the kinetic variables of the scattered partons and the initial and final state radiations.

After all binary collisions are processed, the scattered partons in the associated nucleons are connected with the corresponding valence quarks and diquarks to form string systems. The strings are then fragmented into particles.

The HIJING model incorporate nuclear effects such as parton shadowing and jet quenching. HIJING is designed also to explore the range of possible initial conditions that may occur in nuclear collisions at Cosmic Ray and colliders (RHIC, LHC) energies.

To include the nuclear effects on jet production and fragmentation, the EMC [28] effect of the parton structure functions in nuclei and the interaction of the produced jets with the excited nuclear matter in heavy ion collisions are considered.

It has been observed [28] that the effective number of quarks and antiquarks in a nucleus is depleted in the low region of x . While theoretically there may be differences between quark and gluon shadowing, one assume that the shadowing effects for gluons and quarks are the same.

At this stage, the experimental data unfortunately can not fully determine the A dependence of the shadowing. In the HIJING model the A dependence are taken from Ref. [29]:

$$\begin{aligned}
 R_A(x) &\equiv \frac{f_{a/A}(x)}{Af_{a/N}(x)} \\
 &= 1 + 1.19 \ln^{1/6} A [x^3 - 1.5(x_0 + x_L)x^2 + 3x_0x_Lx] \\
 &\quad - [\alpha_A - \frac{1.08(A^{1/3} - 1)}{\ln(A + 1)} \sqrt{x}] e^{-x^2/x_0^2},
 \end{aligned} \tag{12}$$

$$\alpha_A = 0.1(A^{1/3} - 1), \tag{13}$$

where $x_0 = 0.1$ and $x_L = 0.7$. The term proportional to α_A in Eq. 12 determines the shadowing for $x < x_0$ with the most important nuclear dependence, while the rest gives the overall nuclear effect on the structure function in $x > x_0$ with some very slow A dependence.

To take into account impact parameter dependence, one assume that the shadowing effect α_A is proportional to the longitudinal dimension of the nucleus along the straight trajectory of the interacting nucleons. The values of α_A in Eq. 12 are parametrized like :

$$\alpha_A(r) = 0.1(A^{1/3} - 1) \frac{4}{3} \sqrt{1 - r^2/R_A^2}, \tag{14}$$

where r is the transverse distance of the interacting nucleon from its nucleus center and R_A is the radius of the nucleus. For a sharp sphere nucleus with overlap function $T_A(r) = (3A/2\pi R_A^2) \sqrt{1 - r^2/R_A^2}$, the averaged $\alpha_A(r)$ is $\alpha_A = \pi \int_0^{R_A} dr^2 T_A(r) \alpha_A(r) / A$.

To simplify the calculation during the Monte Carlo simulation, one can decompose $R_A(x, r)$ into two parts,

$$R_A(x, r) \equiv R_A^0(x) - \alpha_A(r)R_A^s(x), \quad (15)$$

where $\alpha_A(r)R_A^s(x)$ is the term proportional to $\alpha_A(r)$ in Eq. 12 with $\alpha_A(r)$ given in Eq. 14 and $R_A^0(x)$ is the rest of $R_A(x, r)$. Both $R_A^0(x)$ and $R_A^s(x)$ are now independent of r .

The effective jet production cross section of a binary nucleon-nucleon interaction in $A+B$ nuclear collisions is then,

$$\sigma_{jet}^{eff}(r_A, r_B) = \sigma_{jet}^0 - \alpha_A(r_A)\sigma_{jet}^A - \alpha_B(r_B)\sigma_{jet}^B + \alpha_A(r_A)\alpha_B(r_B)\sigma_{jet}^{AB}, \quad (16)$$

where σ_{jet}^0 , σ_{jet}^A , σ_{jet}^B and σ_{jet}^{AB} can be calculated through Eq. 1 by multiplying $f_a(x_1, P_T^2)f_b(x_2, P_T^2)$ in the integrand with $R_A^0(x_1)R_B^0(x_2)$, $R_A^s(x_1)R_B^0(x_2)$, $R_A^0(x_1)R_B^s(x_2)$ and $R_A^s(x_1)R_B^s(x_2)$ respectively. With calculated values of σ_{jet}^0 , σ_{jet}^A , σ_{jet}^B and σ_{jet}^{AB} , one get the effective jet cross section σ_{jet}^{eff} for any binary nucleon-nucleon collision.

Another important nuclear effect on the jet production in heavy ion collisions is the final state integration. In high energy heavy ion collisions, a dense hadronic or partonic matter must be produced in the central region. Because this matter can extend over a transverse dimension of at least R_A , jets with large P_T from hard scatterings have to traverse this hot environment. For the purpose of studying the property of the dense matter created during the nucleus-nucleus collisions, HIJING model include an option to model jet quenching in terms of a simple gluon splitting mechanism [12],[13].

The induced radiation in HIJING model is given via a simple collinear gluon splitting scheme with energy loss dE/dz . The energy loss for gluon jets is twice that of quark jets[30]. One assume that interaction only occur with the locally comoving matter in the transverse direction. The interaction points are determined via a probability :

$$dP = \frac{d\ell}{\lambda_s} e^{-\ell/\lambda_s}, \quad (17)$$

with given mean free path λ_s , where ℓ is the distance the jet has traveled after its last interaction. The induced radiation is simulated by transferring a part of the jet energy $\Delta E(\ell) = \ell dE/z$ as a gluon kink to the other string which the jet interacts with. The procedure is repeated until the jet is out of the whole excited system or when the jet energy is smaller than a cutoff below which a jet can not loss energy any more. This cutoff is taken as the same as the cutoff P_0 for jet production. To determine how many and which

excited strings could interact with the jet, one assume a cross section of jet interaction so that excited strings within a cylinder of radius r_s along the jet direction could interact with the jet. λ_s should be related to r_s via the density of the system of excited strings. The values for λ_s and r_s are taken as two parameters in the model.

The main usefulness of these schematic approaches for nuclear shadowing and jet quenching is to test the sensitivity of the final particle spectra .

For a detailed description of the VENUS model as applied in the calculations presented in this paper we refer to excelent review of Werner (sections 6-10) [9].

3 NUMERICAL RESULTS

For used a Monte Carlo generator in Cosmic Ray physics this model should provide the basic hadronic interaction term for the Cosmic Ray cascade i.e should provide the cross sections for hadron-hadron,hadron-nucleus and nucleus-nucleus collisions as function of the energy . Also should provide a good description of secondary particles production since, secondary π^0 and η mesons are the source of the electromagnetic shower , secondary π^\pm and K^\pm mesons are the source of Cosmic Ray Muons and the source of atmospheric Neutrinos produced by Cosmic Ray cascade and secondary charmed mesons are the source for prompt Muons and Neutrinos. The model should work from accelerator energies up to the highest possible primary energies . Experimental observations like rapidity plateaus and average transverse momenta rising with energy,KNO scaling violation,transverse momentum - multiplicity correlations and minijets pointed out that soft hard and processes are closely related and all these properties were understood within the HIJING model [11]-[14].

The HIJING model provides a framework not only for the study of hadron-hadron interactions ,but also for the description of particle production in hadron nucleus and nucleus - nucleus collisions at ultrahigh energies.

The relevance of an event generator like HIJING or VENUS for hadron production cross sections in the Cosmic Ray energy region can only be claimed if the model agrees to the best available data in the accelerator energy range and if it shows a smooth behaviour in the extrapolation to ultrahigher energies .

For the Cosmic Ray Cascade in the atmosphere only hadron - nucleus and nucleus-nucleus collisions are relevant with Nitrogen ^{14}N beeing the most important target nucleus. However experimental data are of much better quality in hadron-hadron,and especially in proton-proton collisions or antiproton-proton collisions than for collisions of hadrons with light nuclei.The scarcity of the data in this region was also pointed out in studing strangeness production at SPS energies [22].

So we start with the study of proton - proton collisions and nucleus - nucleus collisions at accelerator energies .

3.1 PROTON - PROTON AND NUCLEUS-NUCLEUS INTERACTIONS AT ACCELERATOR ENERGIES

We used the program HIJING with default parameters:

1. IHPR2(11)=1 gives the baryon production model with diquark-antidiquark pair production allowed, initial diquark treated as unit;
2. IHPR2(12)=1, decay of particle such as π^0 , K_s^0 , Λ , Σ , Ξ , Ω are allowed ;
3. IHPR2(17)=1 - Gaussian distribution of transverse momentum of the sea quarks ;
4. IHPR2(8)=0 - jet production turned off for theoretical predictions denoted by HIJING model ;
5. IHPR2(8)=10-the maximum number of jet production per nucleon-nucleon interaction for for theoretical predictions denoted by $HIJING^{(j)}$ at SPS energies and 300 GeV ;
6. IHPR2(8)=20 for energies $\geq 1 TeV$. We have neglected also nuclear shadowing effect, and jet quenching (see section 2) and we have a cut in pseudorapidity $\eta > 0.5$ for ultrahigh energies ($\geq 1 TeV$).

In Table I the calculated average multiplicities of particle at $E_{lab} = 200 GeV$ in (pp) interactions are compared to data. The theoretical values as predicted by the model $HIJING$ and $HIJING^{(j)}$ are obtained for 10^5 generated events and in a full phase space. The values $HIJING^{(j)}$ include the very small possibility of mini jet production at these low SPS energies. The experimental data are taken from Gazdzicki and Hansen [32]. The theoretical values given by VENUS model(as computed here) are obtained for 10^4 generated events and in a full phase space. The values labeled DPMJET II are taken from Ranft [5].

The small kaon to pion ratio is due to the suppressed strangeness production basic to string fragmentation. Positive pions and kaons are more abundant than the negative ones due to charge conservation. We note that the *integrated* multiplicities for neutral strange particle $\langle \Lambda \rangle$, $\langle \bar{\Lambda} \rangle$, $\langle K_s^0 \rangle$ are reproduced at the level of three standard deviations for pp interactions at 200 GeV and 300 GeV. (see also Fig.1a and Fig.1b -experimental data from Lo Pinto et al. [33] for pp interactions at 300 GeV.) However the values for $\langle \bar{p} \rangle$ and $\langle \bar{\Lambda} \rangle$ are significantly over predicted by the models.

For completeness we include a comparison of hadron yields at collider energies $E_{LAB} = 160 \text{ TeV}$ for $\bar{p}p$ interactions, where mini-jet production plays a much more important role. From different collider experiments Alner et al. (UA5 Collaboration) [34] attempted to piece together a picture of the composition of a typical soft event at the Fermilab $S\bar{p}\bar{p}S$ collider [35]. The measurements were made in various different kinematic regions and have been extrapolated in the full transverse momenta (p_T) and rapidity range for comparison as described in reference [34]. The experimental data are compared to theoretical values obtained with $HIJING^{(j)}$ in Table II. It was stressed by Ward [35] that the data show a substantial excess of photons compared to the mean value for pions $\langle \pi^+ + \pi^- \rangle$. It was suggested as a possible explanation of such enhancement a gluon Cerenkov radiation emission in hadronic collision [36]. Our calculations rules out such hypothesis. Taking into account decay from resonances and direct gamma production, good agreement is found within the experimental errors.

In the following plots the kinematic variable used to describe single particle properties are the transverse momentum p_T and the rapidity y defined as usual as:

$$y = \frac{1}{2} \ln \frac{E + p_3}{E - p_3} = \ln \frac{E + p_3}{m_T} \quad (18)$$

with E, p_3 , and m_T being energy, longitudinal momentum and transverse mass $m_T = \sqrt{m_0^2 + p_T^2}$ with m_0 being the particle rest mass.

The pseudorapidity η is used rather than the rapidity since for η no knowledge of particle masses is required.

$$\eta = \frac{1}{2} \ln \frac{p + p_3}{p - p_3} = -\ln \tan \frac{\theta}{2} \quad (19)$$

where p is the projectile nucleon momentum and θ is the scattering angle.

Feynman x_F variable is defined for ultrahigh energy as:

$$x_F = 2 \frac{m_T}{\sqrt{s}} \sinh(y^{cm}) \quad (20)$$

where y^{cm} and s are rapidity and total energy in center of mass frame (cms).

In Figure 1 we compare rapidity and transverse momentum distributions for strange particles in proton-proton interactions at 300 GeV given by HIJING model with experimental data [33]. The agreement is quite good. However, it will be interesting to investigate in the

future the Feynman scaling behaviour of the model at the accelerator energies since the forward fragmentation region seems to play an important role [5], [6],[4].

This year marked a real progress in the field of high energy nuclear collisions .Now an entirely new domain of energies has become accessible with heavy nuclear beams [37]. Recently [22] using HIJING and VENUS models the systematics of strangeness enhancement was calculated for pp,pA and AA interactions at SPS energies and it was stressed out that the enhancement of strangeness has its origins in non-equilibrium dynamics of few nucleons systems.To clarify the new physics much better quality data on elementary pp as well as other light ion reactions will be needed for tuned models .

We focused our analyses concerning particle production in nucleus - nucleus interactions at SPS energies , where the models should be better tested ,mainly for two simmetrical interactions $S + S$, $Pb + Pb$ and for asymmetrical one $S + Pb$.

It was shown that the negative pion rapidity densities are well accounted for both HIJING and VENUS [4], but the flat valence proton distribution in $S + S$ is only reproduced by VENUS.Recall that VENUS includes a model of final state interactions in dense matter as well as a colour rope effect ,called double strings.VENUS predicts a much higher degree of baryon stopping at midrapidity than HIJING . These conclusions are confirmed also for our calculations in $S + S$ at 200 $AGeV$ (see Figs. 2a,2b) and $Pb + Pb$ collisions at 160 $AGeV$ (see Figs. 2c,2d) for Λ and $\bar{\Lambda}$. The experimental data are taken from Alber et al. [38]. The rapidity distributions for antiproton \bar{p} and for negative kaons K^- are represented for $S + S$ interactions (Fig.3a(\bar{p}) and Fig.3b(K^-)) and $Pb + Pb$ interactions (Fig.3c(\bar{p}) and Fig.3d (K^-)) in comparison with some experimental data taken from Baechler et al. [39] for K^- and from Murray et al. [40] for \bar{p} . For asymmetrical interactions $S + Pb$ we predict in both models the rapidity spectra for π^- (Fig. 4a) , K^- (Fig. 4b) , Λ (Fig. 4c) and $\bar{\Lambda}$ (Fig. 4d)) at 200 $AGeV$. We mention that we have used VENUS model with the option without decaying resonances (dotted histograms). If will allow decay of resonances then we get an increase of the values especially at mid rapidity which improve agreement between theory and experimental data (dashed histograms).

It will be interesting to compare these results with upcoming data to test if the strangeness enhancement increases from SS to SPb or from SS to $PbPb$ interactions.

3.2 PROTON -AIR NUCLEUS INTERACTIONS AT ULTRA-HIGH ENERGIES

Since not enough data are avaiable in the fragmentation region of hadron collisions with light target nuclei,many features of particles production in collisions involving nuclei can only be extracted from the study of models. These kind of analysis have been done recently

in VENUS model [20] and DPM model [5],[6]. In HIJING model some specific interactions were investigated at RICH and LHC energies [12]-[14].

Taking into account the traditional concept of collisions between nucleons and air nuclei the primary loses its energy during the interaction and this fluctuate between zero and 100 % . The fraction of the energy lost and used for producing new particles is then referred to as inelasticity. We do not investigate traditionally inelasticities (baryonic, electromagnetic or mesonic) see [20].

We generate for proton-Air Nucleus ($p + Air$) interactions 10^4 minimum bias events ($b_{min} = 0, b_{max} = 5fm$). In order to give an idea about energy used for producing new particle we investigate in Figure 5 the transverse energy pseudorapidities spectra and their dependence with energy for all secondaries (Fig. 5a), all neutral (Figure 5b) ,all charged (Fig. 5c) and gluons (Fig. 5d). As we see from Figure 5 gluons carried an important fraction from transverse energy and this fraction increase with increasing energy (from 2.8 % at 1 TeV to 17.3 % at 1000 TeV). Also the percentage of occurrence of gluons increase from 7.20 % at 17.86 TeV to 10.71 % at 1000 TeV (see table 3).

The rapidity distributions and energy dependence of main secondary particles are shown in Figure 6 and Figure 7. Secondary π^\pm (Fig.6a and 6b) and K^\pm (Fig.6c and 6d) are the source of Cosmic Ray Muons and the source of atmospheric Neutrinos produced by the Cosmic Ray cascade. Secondary π^0 (Fig.7a) and η mesons are the source of the electromagnetic shower and secondary charmed mesons (Fig. 7d) are the source for prompt Muons and Neutrinos . The lambdas have been shown (Fig. 7c),because they can be produced from protons by exchanging a single valence quark by strange quark.The outer maximum of their distributions are due to this process.This component is identified in all nucleon distributions (neutron,proton). The statistics (10^4 events generated) seems not to be enough for charmed mesons (D^\pm) but we give such distributions only to show that introducing HIJING code in a shower code with a much higher statistics at simulation level a study of prompt muon component should be feasible.

We see from Figure 6 that mesons distributions exhibit a broad structureless shape which does not depend strongly on the type of mesons but have a dependence on energy from 1 TeV to 1000 TeV which is more pronounced compared with VENUS results (see reference [20].)

More less energy dependence is seen in tranverse momenta distributions for secondaries in p+Air Nucleus interactions in Figure 8(for all charged particles - Fig. 8a, for proton - Fig. 8b, for positive pions π^+ - Fig. 8c and for negative pions π^- -Fig.8d)

Trying to stress out the relevance of accelerator data on particle production in hadron - nucleus collisions for Cosmic Ray cascade we study the Feynman scaling behaviour of

$p + Air \rightarrow \pi^\pm + X$ and $p + Air \rightarrow p + \bar{p} + X$ in Fig.9a and Fig.9b respectively. We plot the $x_F dN/dx_F$ distributions for laboratory energies of 1 TeV (dotted histograms), 100 TeV (dashed histograms), 1000 TeV (solid histograms). The violations of Feynman scaling which occur are connected with known rise of rapidity plateau for all kinds of produced particles and with production of minijets. Due to minijets Feynman scaling is more strongly violated especially in the region $x_F \geq 0$. The violation of Feynman scaling are less dramatic in DPMJET II model [5],[6] and appear only around $x_F = 0$ and $x_F = 1$. We note also that HIJING show violation of KNO scaling due to the production of multiple minijets and the tendency becomes stronger with increasing energy [12].

In order to evaluate multiplicity distributions for the charged particles in $p + Air$ interactions (Fig.10a) we differentiate the contributions from soft (Fig.10b events with $N_{jet} = 0$) and hard processes (Fig.10c events with $N_{jet} = 1$ and Fig.10d events with $N_{jet} > 1$) where N_{jet} is the number of minijets produced in that events. Our calculations including the effects of multiple minijets are the contributions from the events which have hard collisions with $P_T > P_0$. Analysing Figure 10 it is clear that the events at the tails of the charged multiplicity distributions in p+Air interactions are mainly those with multiple minijets production.

3.3 NUCLEUS-AIR NUCLEUS INTERACTIONS AT ULTRA-HIGH ENERGIES

Due to the large fraction of nuclei in primary Cosmic Rays, Nucleus-Air collisions are of great importance in the EAS development. It is important, that the model will be able to give a good description of hadron production in nucleus-nucleus interactions. So, in this subsection we try to investigate mainly the dependence on projectile mass for specific interactions for EAS (He, Ne, S, Fe+Air Nucleus) at 17.86 TeV/Nucleon which correspond to 1 PeV laboratory energy for Fe nucleus.

For a real comparison, the nucleus-nucleus collisions geometry should be the same for all of the Monte Carlo codes since nuclear density distributions are well known from nuclear physics [41]. At SPS energies the calculated number of target and projectile participants as well as the number of participants as a function of reaction impact parameter (b fm) shows no difference in HIJING and VENUS model [4].

The results depicted in Figure 11 are obtained for 10^4 generated events and for the following intervals ($b_{min} - b_{max}$) of impact parameter: Fe+Air (0-13 fm), S+Air(0-11 fm), Ne+Air(0-10 fm), He+Air (0-7 fm) - dotted histograms; Fe+Air (0- 8 fm), S+Air(0-7 fm), Ne+Air(0-6 fm), He+Air (0-5 fm) -dashed histograms; Fe+Air (0 - 5 fm), S+Air(0 - 5 fm), Ne+Air(0 - 5 fm), He+Air (0-4 fm) -solid histograms.

From Figure 11(a,b,c,d) we see that at 17.86 TeV/Nucleon the results have strongly dependence on impact parameter intervals ($b_{min}-b_{max}$) and also the possibility of mixing interactions if we are interested in rapidity spectra only.

Therefore for comparison of HIJING and VENUS results at 17.86 TeV/Nucleon for p+Air,He+Air, Ne+Air,S+Air,Fe+Air and for p+Air at 1000 TeV we try to get approximately the same number of participants. For HIJING model we get the values for mean numbers of participants listed in last lines of Table 3 for 10^4 generated events and the following impact parameter intervals ($b_{min} - b_{max}$): He+Air(0-4 fm),Ne+Air(0-6 fm),S+Air (0-7 fm),Fe+Air (0-8 fm). *p + Air* (0- 5 fm). The results for VENUS model are taken from Schatz et al. [20].

Table 3 lists the frequency of various particles among the secondaries for collisions of different nuclei with nitrogen. Our calculations confirm the results from reference [20] .The percentages do not seem to depend strongly on projectile mass nor,as shown by proton results on energy. We see only a slight tendency of increasing strangeness production with increasing primary mass for VENUS results. Analysing the results of table 3 we see that the VENUS model predict more pions and kaons , but less gamma particles that HIJING model . We remark also differences in total multiplicities at ultrahigh energy which can not be explained only by the difference between total number of participants . It seems that *"double string" mechanism change considerably the baryon spectra and allows the baryon number to migrate several units of rapidity from the end point rapidity.*

Important for Cosmic Ray studies and EAS development is also the dependence of particle production on the nuclear target and projectile. Taken into consideration the same conditions as those reported for the values listed in Table 3 the theoretical predictions for mass dependence of pseudorapidities spectra are given for transverse energy in Figure 12, for transverse momenta in Figure 13 and for main secondaries produced new particles in Figure 14. The transverse momenta distributions of all charged, proton, π^+,π^- are represented in Figure 15. For Feynman $x_F dN/dx_F$ distributions we give theoretical values for specific EAS interactions in Figure 16 only for charged pions and for sum of protons and antiprotons . We see a slight mass dependence of Feynman distributions and transverse momenta distributions for $A \geq 20$.

Instead of the proper sampling of Nucleus + Air Nucleus scattering events , an approximation often applied in EAS development is the so called superposition model. There are two different possible superposition models: a nucleus-nucleus collision A-B with N_{part} participating nucleons is approximated as the superposition of N_{part} simultaneous nucleon-nucleon collisions and the second one : a nucleus-nucleus collision A-B with N_{proj} participating projectile nucleons is approximated as the superposition of N_{proj} simultaneous nucleon-B

collisions. The validity of this principle was analysed in some recent works [20], [5],[6] with different conclusions.

We investigate in HIJING model the integrated mean transverse energy for secondaries produced in Nucleus+Air Nucleus interactions at 17.86 TeV/Nucleon. So,we generate 10^4 events in the same impact parameter interval (0-5 fm) for Fe,S,Ne,He,p+Air interactions. The values obtained for mean projectile participants (N_{proj}) and mean number of binary collisions N_{coll} (which include nucleon-nucleon($N-N$), nucleon-wounded nucleon($N-N_w$), N_w-N and $N_w - N_w$ collisions) are listed in Table 4. The results given in Table 4 are for all secondaries , all charged and all neutrals particles produced in interactions. The values of integrated mean transverse energy $\langle E_T \rangle$ scale with number of binary collisions in nucleus-nucleus interactions at this energy N_{coll} and scaling proprietes are valid for $A \geq 20$ and should not be applied to lighth nucleus+Air interactions. Since integrated mean value of transverse energy $\langle E_T \rangle$ is a measurable quantity it will be interesting to verify this scaling at RHIC energies.

In order to evaluate multiplicity distributions for charged particles in A+Air interactions we differentiate the contribution for all events (soft + hard) (Fig.17a for Fe+Air and Fig.17b for S+Air) and only hard processes - events with $N_{jet} > 1$ (Fig.17c for Fe+Air and Fig.17d for S+Air). We can see from Figure 17 that the low multiplicity events are dominated by those of no jet production while high multiplicity events are dominated by those of at least one jet production. Also it is clear from Figure 17 that the contributions from the events which have hard collisions increase with increasing of available energy and of projectile mass.

At ultrahigh energies nuclear effects like nuclear shadowing of partons and jet quenching (see section 2) , should have important contributions [12],[13]. In HIJING model a simple parametrisation of gluon shadowing (see eqs 12-15) and a schematic quenching model (see eqs 16-17) were introduced to test the sensitivity of the final distributions to these aspects of nuclear dynamics. Trying to estimate the results taken into consideration and neglected such effects we expect biggest differences for more central Fe+Air interactions at 17.86 TeV/Nucleon.Therefore we will estimate these effects for impact parameter interval(0 – 5fm)). In Figure 18 we give theoretical values for pseudorapidity distributions for charged pions (Fig.18a and Fig.18b) and for charged kaons (Fig.18c and Fig.18d) without parton shadowing and jet quenching (solid histograms) and with parton shadowing and jet quenching(dashed histograms). The quenching mechanism in HIJING is limited to $p_T > 2 GeV/c$ partons. For pseudorapidity distributions of main secondary particles produced in EAS specific interactions in this energy region these effects should be neglected.

However ,these effects are more pronunciated at the early stage of collisions ,like we see from Figure 19 which depicted pseudorapidity distributions for gluons (Fig.19a) and quark-

antiquark pairs(Fig.19b) as well as transverse momenta distributions for valence and sea partons (Fig.19c) and valence parton only (Fig.19d). Of great importance are also energy densities which are produced in these interactions ,at the early collisions time but their values are under study now.

4 Conclusions

In this paper we have performed an analysis of particle production in pp and AA collisions at SPS CERN-energies using the HIJING and VENUS models and investigate possible applications of the models at Cosmic Ray energies mainly for p+Air Nucleus at 1 TeV ,10 TeV, 1000 TeV and Nucleus-Air Nucleus interactions (Fe,S,Ne,He+Air,p+Air) at 17.86 TeV/Nucleon .

We stressed out that integrated multiplicities are quite well reproduced at the level of three standard deviations for pp interaction at 200 GeV and 300 GeV. However the values for $\langle \bar{p} \rangle$ and $\langle \bar{\Lambda} \rangle$ are significantly overpredicted by the models. A very good agreement is found within experimental errors for ultrahigh energies (160 TeV) in HIJING approach where mini-jet production plays a much more important role.

For nucleus-nucleus collisions at SPS energies the rapidity spectra are well accounted for both HIJING and VENUS models for mesons ,but VENUS model seems to give a more good description for strangeness production.At SPS energies a final state interactions in dense matter as well as a colour rope effect predicts much higher degree of baryon stopping at midrapidity than HIJING.

The event generator VENUS [20] and HIJING in the present study were tested to simulate ultrahigh energy collisions specific for EAS development. The transverse energy,transverse momenta and secondary particles produced spectra as well as their energy and mass dependences were investigated in detail.

The contributions from the events which have hard collisions are stongly evidentiated at the tail of charged particles multiplicity distributions and increase with increasing energy and increasing mass of projectile. Feynman scaling is strongly violeted in HIJING model due to multiple minijets events. For Cosmic Ray energy region and specific EAS interactions the effects of parton shadowing and jet quenching should be neglected.

Possible utilization inside a shower code of these models allows to extend the analyses and to release the simple superposition model which is not valid at least for integrated mean transverse energy of secondaries particle . The thoretical values predicted by HIJING model suggest a scaling with number of binary nucleon-nucleon collisions. It will be interesting to verify this hypothesis in the future experiments at RHIC energies.

5 Acknowledgements

We are grateful to Klaus Werner for providing us the source code of VENUS. One of the authors (VTP) would like to express his gratitude to Professor C.Voci and Professor M.Morando for kind invitation and acknowledge financial support from INFN-Sezione di Padova, Italy where part of the presented calculations were performed. VTP is also indebted to Professor T. Ludlam and M.Gyulassy for kind financial help and hospitality during his stay in Columbia University, New York and to Dr. Xin Niang Wang for very useful discussions on different aspects of HIJING model. He acknowledges also financial support from FZK-Karlsruhe, Germany where this work was finished.

References

- [1] H.Rebel in *Topics in Atomic and Nuclear Collisions (NATO ASI Series B321*,eds. B.Rемаud , A. Calboreanu and V. Zoran (New Plenum),p397, (1994)
- [2] D.Muller,S.P.Swordy,P.Meyer,L.Heureux and J.M. Grunsfeld , *Astrophys.J.***374** (1991) 356
S.P.Swordy,L.Heureux,P.Meyer and D.Muller, *Astrophys.J.***403** (1993) 658
- [3] A.Haungs,J. Kempa,H.J. Mathes,H. Rebel,J. Wentz
Preprint submitted to Elsevier Science (July 1995)
- [4] M.Gyulassy and V.Topor Pop ,Preperint CU- 95 (in preparation)
- [5] J.Ranft,Preprint LNF-94/035(P),Laboratori Nazionali di Frascati (Submitted to *Phys.Rev.D*)
- [6] G.Battistoni,C.Forti,J.Ranft, Preprint LNF-94/048, Laboratori Nazionali di Frascati ;
Astroparticle Physics **3** (1995) 157
- [7] A.Capella,U.Sukhatme,C. I. Tan and J. Tran Thanh Van ,*Phys. Rep.***236**,225(1994)
- [8] N. S. Amelin ,E.F.Staubo,L.P.Csernai,V.D.Toneev,K.K.Gudima,
*Phys.Rev.***C44**,1541(1991)
N. S. Amelin,L.V.Bravina,L.P.Csernai,V.D.Toneev K.K.Gudima,S.Yu. Sivoklokov,
*Phys.Rev.***C47**,2299(1993)
- [9] K. Werner,Preprint HD-TVP-93-1(1993),University of Heidelberg,Germany;
*Phys.Rep.***232**,87(1993)
- [10] B.Andersson,G.Gustafson and Nilsson-Almqvist *Nucl.Phys.***B281**,289(1987);
B.Nilsson-Almqvistand E.Stenlund, *Comp.Phys.Commun.***43**,387(1987)
- [11] Xin-Nian Wang and Miklos Gyulassy, *Comp.Phys.Comm.***83**,307(1994)
- [12] Xin-Nian Wang,*Phys.Rev.***D43**,104(1991)
- [13] Xin-Nian Wang and Miklos Gyulassy,*Phys.Rev.* **D44**,3501(1991)
- [14] Xin-Nian Wang and Miklos Gyulassy,*Phys.Rev.* **D45**,844(1992)
- [15] K.Geiger,*Phys.Rep.* **258**, 237 (1995)

- [16] N.S.Amelin,H.Stocker,W.Greiner, N. Armesto,
M.A. Braun and C. Pajares,Phys.Rev. **C52**,362, (1995)
- [17] J. N. Capdevielle ,J. Phys. **G:Nucl.Phys.** **15** (1989) 909
- [18] C.Forti,H. Biloken,B.Piazzoli,T.K.Gaisser, L. Satta and T. Stanev, Phys.Rev.**D42**
(1990) 3668
- [19] R.S.Fletcher,T.K. Gaisser,P. Lipari and T.Stanev,Bartol Preprint BA 94-01,submitted
to Phys. Rev. D (1994)
- [20] G. Schatz,T. Thouw,K. Werner,J. Oehlschlager and K. Bekk ,J. Phys. G:
Nucl. Part. Phys.**20**(1994)1267
- [21] J. N. Capdevielle et al., KFK Report **4998**,Kernforschungszentrum Karlsruhe (1992)
- [22] V.Topor Pop,M.Gyulassy,X.N.Wang,A.Andrighetto, M.Morando,F.Pellegrini,
R.A.Ricci,G.Segato , Preprint CU-676(1995),Columbia University,New York,
Phys.Rev.C (in print)
- [23] T.Sjostrand,Comp.Phys.Comm.**82**,74(1994)
- [24] A. Capella and J. Tran Thanh Van, Z. Phys. **C 23**,165 (1984); T. K. Gaisser and
F. Halzen, Phys. Rev. Lett. **54**,1754 (1985); G. Pancheri and Y. N. Srivastava, Phys.
Lett. **182B**, 199 (1986); L. Durand and H. Pi, Phys. Rev. Lett. **58**, 303 (1987)
- [25] K. J. Eskola, K. Kajantie and J. Lindfors, Nucl. Phys. **B323**, 37 (1989)
- [26] E. Eichten, I. Hinchliffe and C. Quigg, Rev. Mod. Phys. **56**, 579 (1984).
- [27] D. W. Duke and J. F. Owens, Phys. Rev. **D 30**, 50 (1984).
- [28] EM Collab., J. Ashman, *et al.*, Phys. Lett. **202B**, 603 (1988); EM Collab., M. Arneodo,
et al., Phys. Lett. **211B**, 493 (1988).
- [29] A. H. Mueller and J. Qiu, Nucl. Phys. **B 268**, 427 (1986); J. Qiu, Nucl. Phys. **B 291**,
746 (1987).
- [30] M. Gyulassy and X. N. Wang, preprint LBL-32682.
- [31] H.H.Mielke,M.Foller,J.Engler and J.Knapp, J.Phys.**G**;
Nucl.Part.Phys. **20**(1994)637
- [32] M.Gazdzicki and O.Hansen,Nucl.Phys.**A528**(1991),754

- [33] F.Lo Pinto et al., Phys.Rev. **D22**, 573 (1980)
- [34] G.J.Alner et al.,Phys.Rep.**154**,247(1987)
- [35] D. R. Ward *Properties of Soft Proton Antiproton Collisions* in Advances Series on Direction in High Energy Physics ,Vol.4 ,Eds.G.Altarelli and L.Di Lella,1989 ,p.85
- [36] I. M. Dremin ,Sov.J.Nucl.Phys. **33**,726(1981)
- [37] M.Gyulassy in Proc.of Eleventh International Conference on Ultrarelativistic Nucleus-Nucleus Collisions, Quark Matter '95 (Monterey,California,USA 9-13 January,1995), edited by A.M.Poskanzer, J.W.Harris and L.S.Schroder Nucl.Phys.**A590** , 431c (1995)
- [38] T.Alber et al.,Z.für Physik **C64**(1994)195
- [39] J.Baechler et al.,Z.für Physik **C58** (1993) 367
- [40] M.Murray et al., Proc.of International Workshop *Strangeness in Hadronic Matter*, January 4-7 ,1995,Tucson,Arizona (to be published) (private communication)
- [41] T.C.Awes,S.P.Sorensen , Nucl.Phys.**A498**, 123c(1989).

Figure Captions

Figure 1: Rapidity (Fig.1a) and transverse momenta(Fig.1b) distributions of Λ^0 (dotted histograms), $\bar{\Lambda}^0$ (dashed histograms), and K_S^0 (full histograms) produced in pp interactions at 300 GeV . HIJING results are shown by histograms. The experimental data are taken from [33].

Figure 2: Rapidity distributions of Λ and $\bar{\Lambda}$ produced in central SS collisions at 200 AGeV (Fig.2a and Fig.2b) respectively and in central $PbPb$ collisions at 160 AGeV (Fig.2c and Fig.2d respectively).Expectations based on HIJING model are depicted as solid histograms . The theoretical predictions based on VENUS model are depicted as dotted histograms (option without decaying of resonances) and as dashed histograms (option with decay of resonances). The NA35 data (full circles) are from Alber et al. [38]. The open circles show the distributions for SS collisions reflected at $y_{lab} = 3.0$.

Figure 3: Comparison of central $S + S$ collisions at 200 AGeV (Fig.3a -antiproton and Fig.3b - negative kaons) with central $PbPb$ collisions at 160 AGeV (Fig.3c-antiproton and Fig.3d- negative kaons). The experimental data are from NA44 [40] for antiprotons and from [39] for negative kaons. The open circles show the distributions for SS collisions reflected at $y_{lab} = 3.0$. The solid,dashed and dotted histograms have the same meaning as in Figure 2.

Figure 4: The various theoretical predictions for $S + Pb \rightarrow \pi^- + X$ (Fig.4a), $S + Pb \rightarrow K^- + X$ (Fig.4b), $S + Pb \rightarrow \Lambda + X$ (Fig.4c) and $S + Pb \rightarrow \bar{\Lambda} + X$ (Fig.4d) at 200 AGeV. The solid and dotted histograms have the same meaning as in Figure 2.

Figure 5: Pseudorapidity distributions for transverse energy of secondary produced particles: all secondaries (Fig.5a) , all neutrals(Fig-5b) , all charged (Fig.5c) and gluons (Fig.5d) in $p + Air$ Nucleus interactions . The dotted(for 1 TeV laboratory energy) , dashed(for 100 TeV laboratory energy), and solid(for 1000 TeV laboratory energy) histograms are theoretical values given by HIJING model.

Figure 6: Pseudorapidity distributions for $p + Air \rightarrow \pi^+ + X$ (Fig.6a), $p + Air \rightarrow \pi^- + X$ (Fig.6b), $p + Air \rightarrow K^+ + X$ (Fig.6c), $p + Air \rightarrow K^- + X$ (Fig.6d) , at 1 TeV,100 TeV and 1000 TeV. The dotted ,dashed and solid histograms have the same meaning as in Figure 5.

Figure 7: Pseudorapidity distributions for $p + Air \rightarrow \pi^0 + X$ (Fig.7a), $p + Air \rightarrow \gamma + X$ (Fig.7b), $p + Air \rightarrow \Lambda^0 + X$ (Fig.7c), $p + Air \rightarrow D^\pm + X$ (Fig.7d),at 1 TeV,100 TeV and 1000 TeV. The dotted ,dashed and solid histograms have the same meaning as in Figure 5.

Figure 8: Transverse momenta distributions for $p + Air \rightarrow all\ charged + X$ (Fig.8a), $p + Air \rightarrow p + X$ (Fig.8b), $p + Air \rightarrow \gamma + X$ (Fig.8c), $p + Air \rightarrow \bar{p} + X$ (Fig.8d), at 1 TeV,100 TeV and 1000 TeV. The dotted ,dashed and solid histograms have the same meaning as in Figure 5.

Figure 9: Test of Feynman scaling in the production of $p + Air \rightarrow \pi^\pm + X$ collisions (Fig.9a) and $p + Air \rightarrow p + \bar{p} + X$ collisions (Fig.9b), between 1 TeV - 1000 TeV. The Feynman $-x_F$ distributions were calculated with HIJING model. The dotted ,dashed and solid histograms have the same meaning as in Figure 5.

Figure 10: Charged multiplicities distributions in $p + Air$ interactions at 1000 TeV.Contibutions from all events are depicted in Fig.10a. In Fig.10b the histogram is from HIJING model calculations with contributions from events with $N_{jet} = 0$, Fig.10c the histogram is from calculations with contributions from events with $N_{jet} = 1$ and in Fig.10d the histogram is from calculations with contributions from events with $N_{jet} > 1$.

Figure 11: Pseudorapidity distributions for all secondaries produced in Fe+Air interactions(Fig.11a),S+Air interactions(Fig.11b), Ne+Air interactions(Fig.11c)and He+Air interactions (Fig.11d) at 17.86 TeV/Nucleon for events generated in different impact parameters intervals (b_{min}, b_{max}). See the text for explanations.

Figure 12: Pseudorapidity distributions for transverse energy of secondary produced particles :all secondaries(Fig.12a); all neutrals(Fig.12b);all charged(Fig.12c);gluons(Fig.12d) in $A + Air$ interactions at 17.86 TeV/Nucleon. The theoretical values were calculated with HIJING model and are depicted by dotted (He+Air) ; dot-dashed (Ne+Air) ; dashed (S+Air) and solid (Fe+Air) histograms.

Figure 13: Pseudorapidity distributions for transverse momenta of secondary particles for $A + Air \rightarrow \pi^\pm + X$ (Fig.13a) and $A + Air \rightarrow p + X$ colisions (Fig.13b) at 17.86 TeV/Nucleon. The histograms have the same meaning as in Figure 12.

Figure 14: Pseudorapidity distributions for $A + Air \rightarrow \pi^+ + X$ (Fig.14a), $A + Air \rightarrow \pi^- + X$ (Fig.14b), $A + Air \rightarrow K^+ + X$ (Fig.14c), $A + Air \rightarrow K^- + X$ (Fig.14d), at 17.86 TeV/Nucleon. The histograms have the same meaning as in Figure 12.

Figure 15: Transverse momenta distributions for $A + Air \rightarrow all\ charged + X$ (Fig.15a), $A + Air \rightarrow p + X$ (Fig.15b), $A + Air \rightarrow \pi^+ + X$ (Fig.15c), $A + Air \rightarrow \pi^- + X$ (Fig.15d),at 17.86 TeV/Nucleon. The histograms have the same meaning as in Figure 12.

Figure 16: The Feynman x_F distributions in the production of $A + Air \rightarrow \pi^\pm + X$ collisions (Fig.16a) and $A + Air \rightarrow p + \bar{p} + X$ colisions(Fig.16b), at 17.86 TeV/Nucleon. The histograms have the same meaning as in Figure 12 .

Figure 17: Charged particles multiplicities distributions in Fe+Air interactions (Fig.17a) and S+Air interactions (Fig.17b) at 17.86 TeV/Nucleon. Contributions from events with number of minijets $N_{jet} > 1$ are represented in Fig.17c for Fe+Air interactions and in Fig.17d for S+Air interactions.

Figure 18: Pseudorapidity distributions for $Fe + Air \rightarrow \pi^+ + X$ (Fig.18a), $Fe + Air \rightarrow \pi^- + X$ (Fig.18b), $Fe + Air \rightarrow K^+ + X$ (Fig.18c), $Fe + Air \rightarrow K^- + X$ (Fig.18d) at 17.86 TeV/Nucleon and impact parameter interval (0-5 fm). Solid histograms are HIJING model predictions.Also showing the influence of nuclear shadowing and jet quenching effects (dashed histograms).

Figure 19: Rapidity distributions for gluons (Fig.19a) and quark-antiquark pairs ($q\bar{q}$) (Fig.19b), transverse momenta distributions for valence and sea partons (Fig.19c) and valence parton (Fig.19d) for Fe+Air interactions at 17.86 TeV/Nucleon and impact parameter interval (0-5 fm). The solid and dashed histograms have the same meaning as in Figure 18.

Table 1: Particle multiplicities for pp interaction at 200 GeV are compared with data from Gazdzicki and Hansen [32] and with the results given by VENUS model (as computed here) and DPM model DPMJET II [5].

pp	Exp.data	HIJING	HIJING ^(j)	VENUS	DPMJET II
$\langle \pi^- \rangle$	2.62 ± 0.06	2.61	2.65	2.60	2.56
$\langle \pi^+ \rangle$	3.22 ± 0.12	3.18	3.23	3.10	3.17
$\langle \pi^0 \rangle$	3.34 ± 0.24	3.27	3.27	3.28	3.38
$\langle h^- \rangle$	2.86 ± 0.05	2.99	3.03	3.05	2.82
$\langle K^+ \rangle$	0.28 ± 0.06	0.32	0.32	0.27	0.28
$\langle K^- \rangle$	0.18 ± 0.05	0.24	0.25	0.19	0.19
$\langle \Lambda + \Sigma^0 \rangle$	0.096 ± 0.015	0.16	0.165	0.18	
$\langle \Lambda + \Sigma^0 \rangle$	0.013 ± 0.01	0.03	0.037	0.033	
$\langle K_s^0 \rangle$	0.17 ± 0.01	0.26	0.27	0.27	0.22
$\langle p \rangle$	1.34 ± 0.15	1.43	1.45	1.35	1.34
$\langle \bar{p} \rangle$	0.05 ± 0.02	0.11	0.12	0.06	0.07

Table 2: Particle composition of $p + \bar{p}$ interactions at 540 GeV in cms.

Particle type	$\langle n \rangle$	Exp.data	HIJING ^(j)
All charged	29.4 ± 0.3	[34]	28.2
$\mathbf{K}^0 + \mathbf{K}^0$	2.24 ± 0.16	[34]	1.98
$\mathbf{K}^+ + \mathbf{K}^-$	2.24 ± 0.16	[34]	2.06
$\mathbf{p} + \bar{\mathbf{p}}$	1.45 ± 0.15	[35]	1.55
$\mathbf{\Lambda} + \bar{\mathbf{\Lambda}}$	0.53 ± 0.11	[34]	0.50
$\mathbf{\Sigma}^+ + \mathbf{\Sigma}^- + \mathbf{\Sigma}^+ + \mathbf{\Sigma}^-$	0.27 ± 0.06	[35]	0.23
$\mathbf{\Xi}^-$	0.04 ± 0.01	[34]	0.037
γ	33 ± 3	[34]	29.02
$\pi^+ + \pi^-$	23.9 ± 0.4	[34]	23.29
\mathbf{K}_s^0	1.1 ± 0.1	[34]	0.99
π^0	11.0 ± 0.4	[35]	13.36

Table 3: Percentage of occurrence of various particles among the secondaries of a Nucleus-Air collision as calculated by the HIJING and VENUS models. The number of protons and neutrons have been reduced by respective numbers in the primary system (values labeled by star(*) [20]). The average multiplicity and numbers of participants are also given .

Particle type	Projectile Energy(TeV/N)	⁵⁶ Fe 17.86	³² S 17.86	²⁰ Ne 17.86	⁴ He 17.86	p 17.86	p 1000
$\langle \pi^- + \pi^+ \rangle$	HIJING	45.98	45.93	45.96	45.86	45.76	46.57
	VENUS	51.02	51.29	51.48	52.34	53.05	52.15
$\langle \pi^0 \rangle$	HIJING	26.13	26.02	26.10	25.93	26.04	26.38
	VENUS	28.30	28.52	28.49	28.85	28.93	28.43
$\langle K^+ + K^- \rangle$ K mesons	HIJING	5.20	5.20	5.20	5.20	5.16	5.58
	VENUS	12.35	12.02	11.84	11.11	10.51	10.86
$\langle K_s^0 \rangle$	HIJING	2.54	2.57	2.53	2.52	2.57	2.75
	VENUS						
$\langle p \rangle$ $\langle p \rangle^*$	HIJING	4.16	4.20	4.20	4.37	4.78	3.25
	VENUS	0.70	0.66	0.66	0.66	-0.11	0.66
$\langle n \rangle$ $\langle n \rangle^*$	HIJING	4.12	4.20	4.23	4.40	4.16	2.86
	VENUS	0.54	0.61	0.64	0.66	1.49	1.43
$\langle \Lambda \rangle$ $\langle \Lambda + \Sigma^0 \rangle$	HIJING	0.70	0.70	0.71	0.72	0.72	0.56
	VENUS	1.66	1.64	1.67	1.60	1.55	1.31
Other baryons	HIJING						
	VENUS	0.46	0.43	0.42	0.34	0.26	0.28
$\langle \gamma \rangle$	HIJING	4.30	4.30	4.33	4.23	4.27	4.48
	VENUS	1.60	1.48	1.43	1.20	1.12	1.18
all charged	HIJING	57.30	57.47	57.54	57.54	57.84	57.79
all neutrals	HIJING	42.33	42.57	42.61	42.50	42.40	42.18
$\langle \bar{p} \rangle$	HIJING	1.42	1.38	1.43	1.40	1.41	1.56
$\langle \bar{n} \rangle$	HIJING	1.40	1.38	1.43	1.40	1.41	1.60
$\langle \text{gluons} \rangle$	HIJING	9.70	9.20	8.96	7.73	7.20	10.71
$\langle q + \bar{q} \rangle$	HIJING	0.40	0.43	0.41	0.36	0.33	0.71
Mean multiplicity	HIJING	274.0	217.5	203.0	88.7	38.9	51.7
	VENUS	354.7	270.5	209.3	92.6	49.4	106.5
Mean projectile participants	HIJING	9.6	7.2	6.5	2.2	1.0	1.0
	VENUS	12.1	8.1	5.7	2.1	1.0	1.0
Mean target participants	HIJING	5.9	5.6	5.6	3.4	2.06	1.42
	VENUS	6.0	5.3	4.7	3.2	2.0	2.06

Table 4: Mean transverse energy for the secondaries of a Nucleus-Air collisions at 17.86 TeV/Nucleon as calculated by the HIJING model and by considering superposition of N_{coll} nucleon-nucleus collisions and N_{proj} nucleon-nucleus collisions, where N_{coll} is the number of binary collisions and N_{proj} is the number of participant projectile nucleons. E_T^{pA} is mean transverse energy in p+Air interaction at the same energy and in the same impact parameter interval (see the text for explanation).

	Projectile	^{56}Fe	^{32}S	^{20}Ne	^4He	p
Mean number	$\langle N_{coll} \rangle$	27.75	19.21	13.61	2.62	
Mean number	$\langle N_{proj} \rangle$	18.43	11.44	8.24	1.73	
Mean Transverse Energy (GeV)	all secondaries	212.5	140.7	104.2	25.16	7.54
	$N_{coll} * E_T^{pA}$	209.2	144.8	102.6	19.75	
	$N_{proj} * E_T^{pA}$	138.96	86.25	62.10	13.04	
Mean Transverse Energy (GeV)	all charged	122.7	81.27	60.10	14.52	4.39
	$N_{coll} * E_T^{pA}$	121.8	84.33	59.74	11.50	
	$N_{proj} * E_T^{pA}$	80.90	50.22	36.17	7.6	
Mean Transverse Energy (GeV)	all neutrals	89.87	59.43	44.10	10.64	3.15
	$N_{coll} * E_T^{pA}$	87.41	60.51	42.87	8.25	
	$N_{proj} * E_T^{pA}$	58.05	36.03	25.95	5.44	

P+P(300 GeV) RAPIDITY AND TRANSVERSE MOMENTUM HIJING

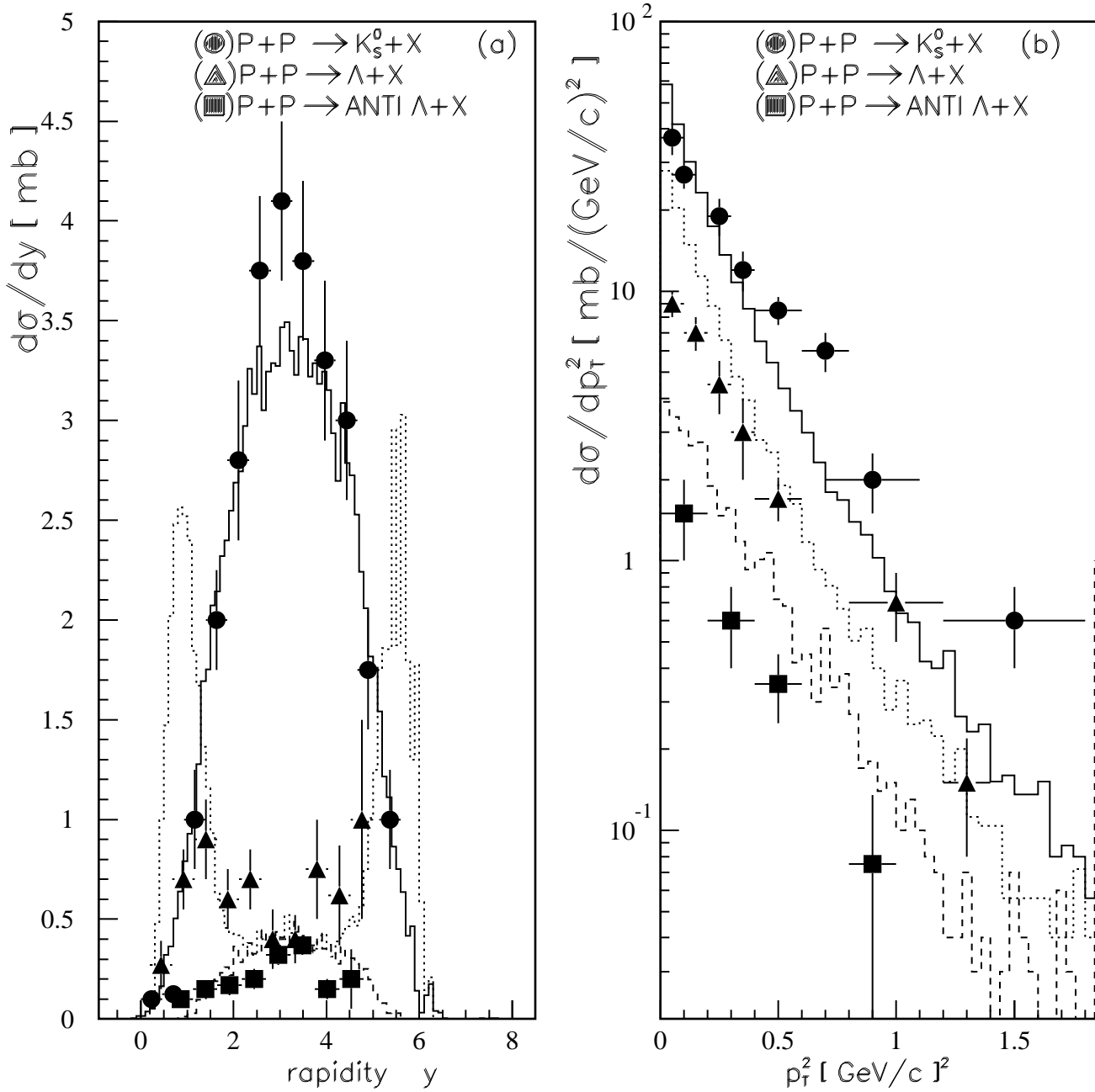


Figure 1

S+S(200 AGeV),Pb+Pb(160 AGeV)(b=0-1 fm) Hijing(-) vs.Venus(- -)

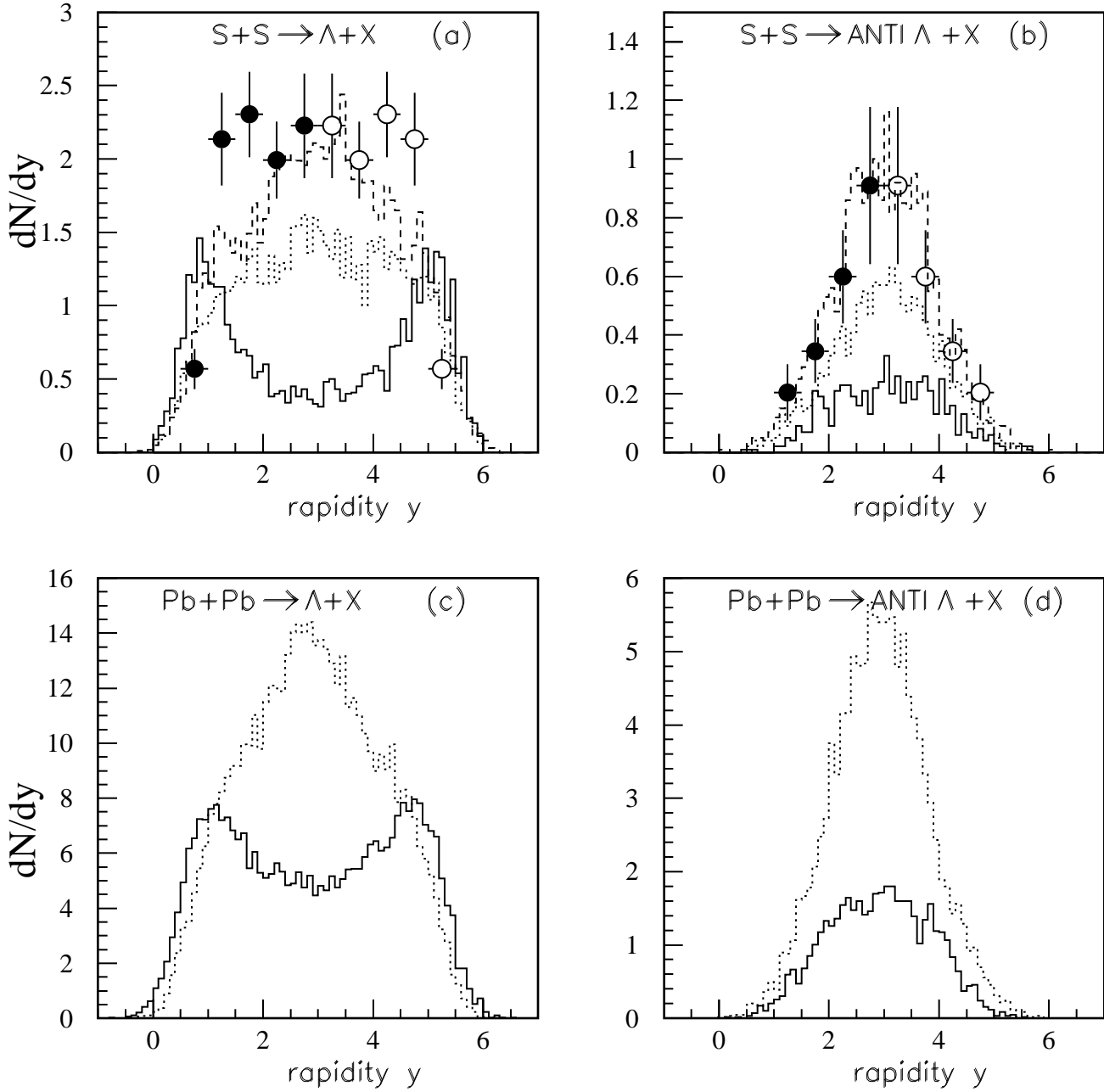


Figure 2

S+S(200 AGeV),Pb+Pb(160 AGeV)(b=0-1 fm) Hijing(-) vs.Venus(- -)

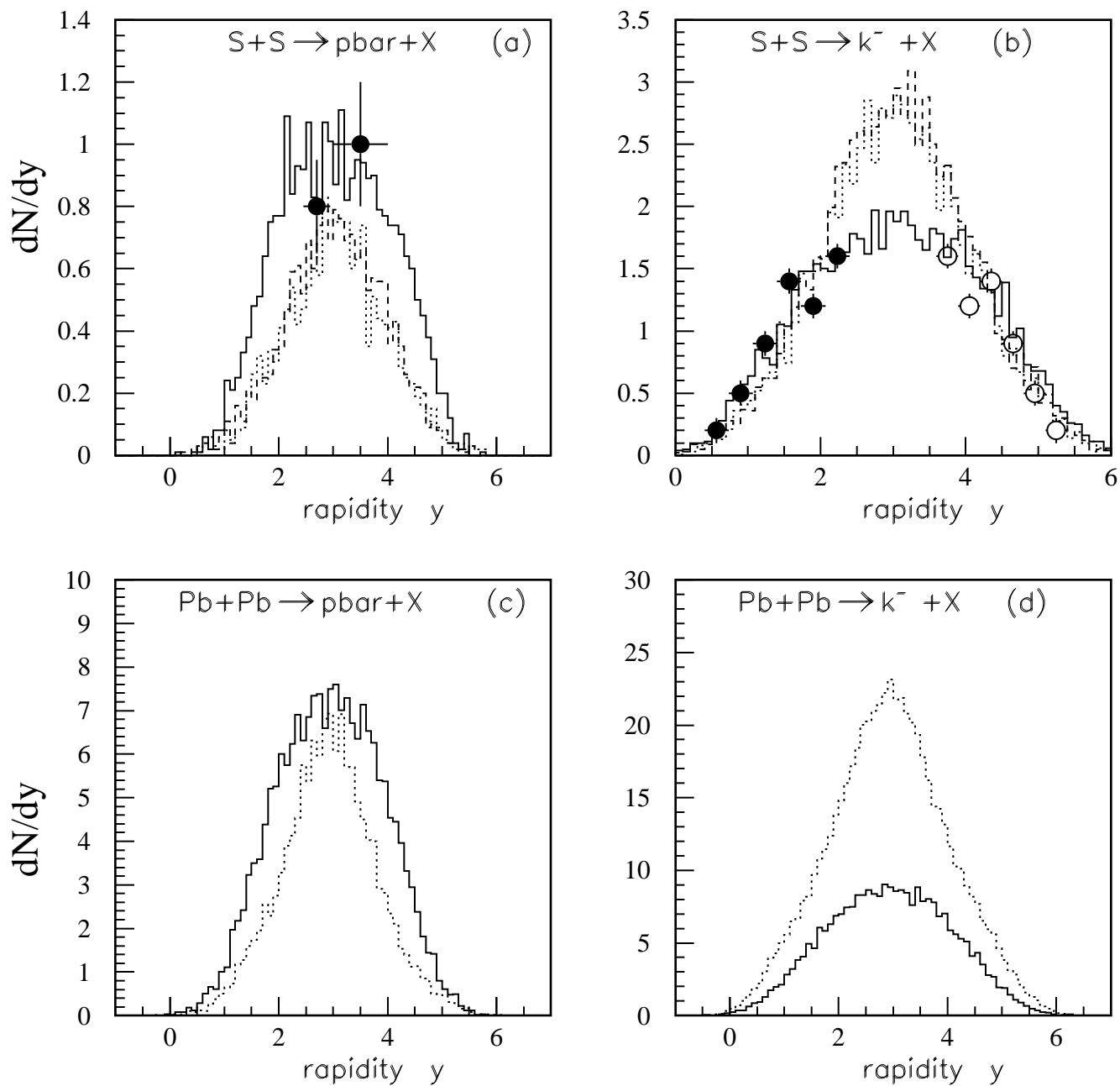


Figure 3

S+Pb(200 AGeV, $b=0-1$ fm) Hijing (—) vs. Venus(---)

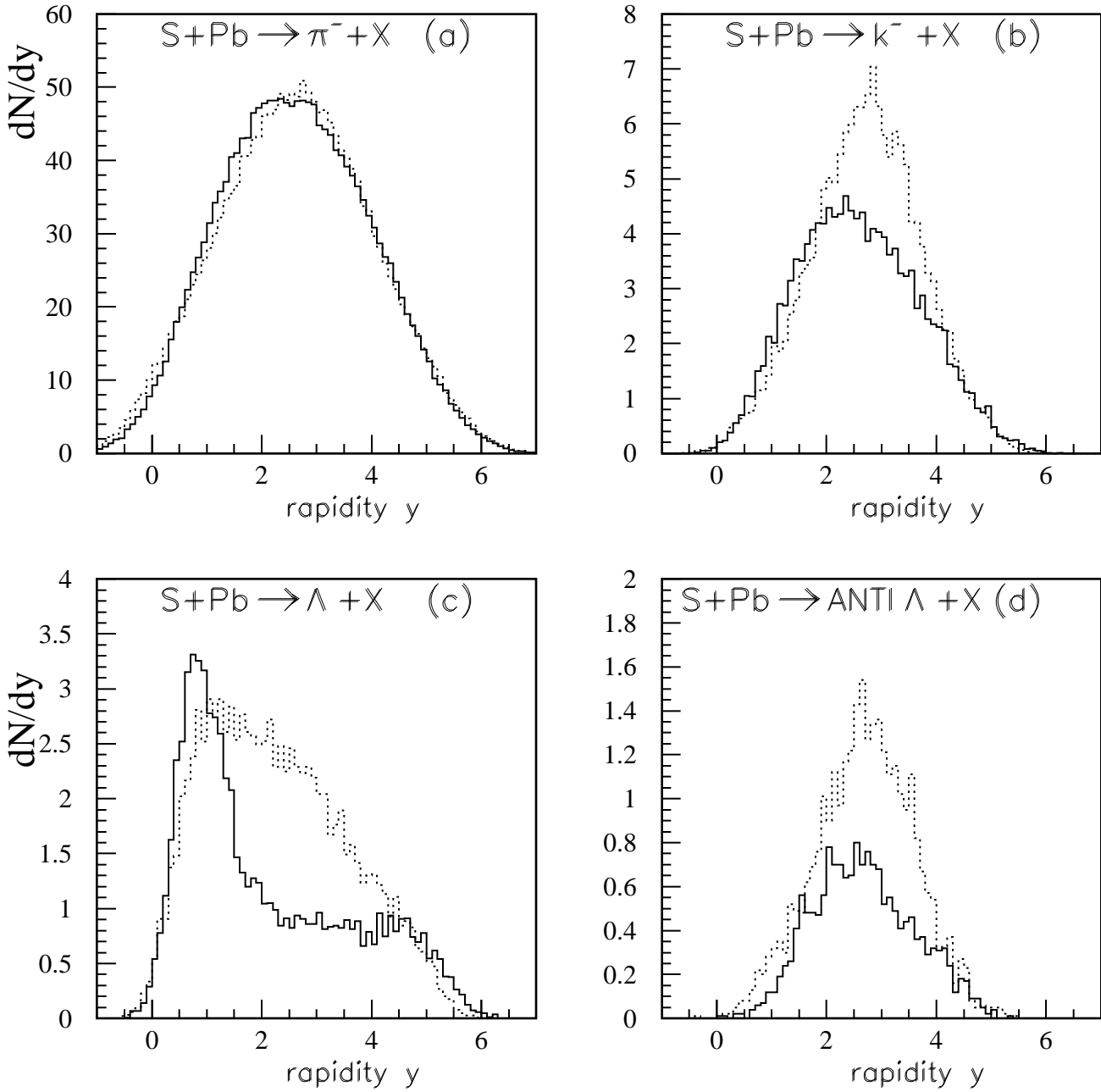


Figure 4

p+Air 1 TeV–1000 TeV 10^4 events ($b=0-5$ fm) HIJING

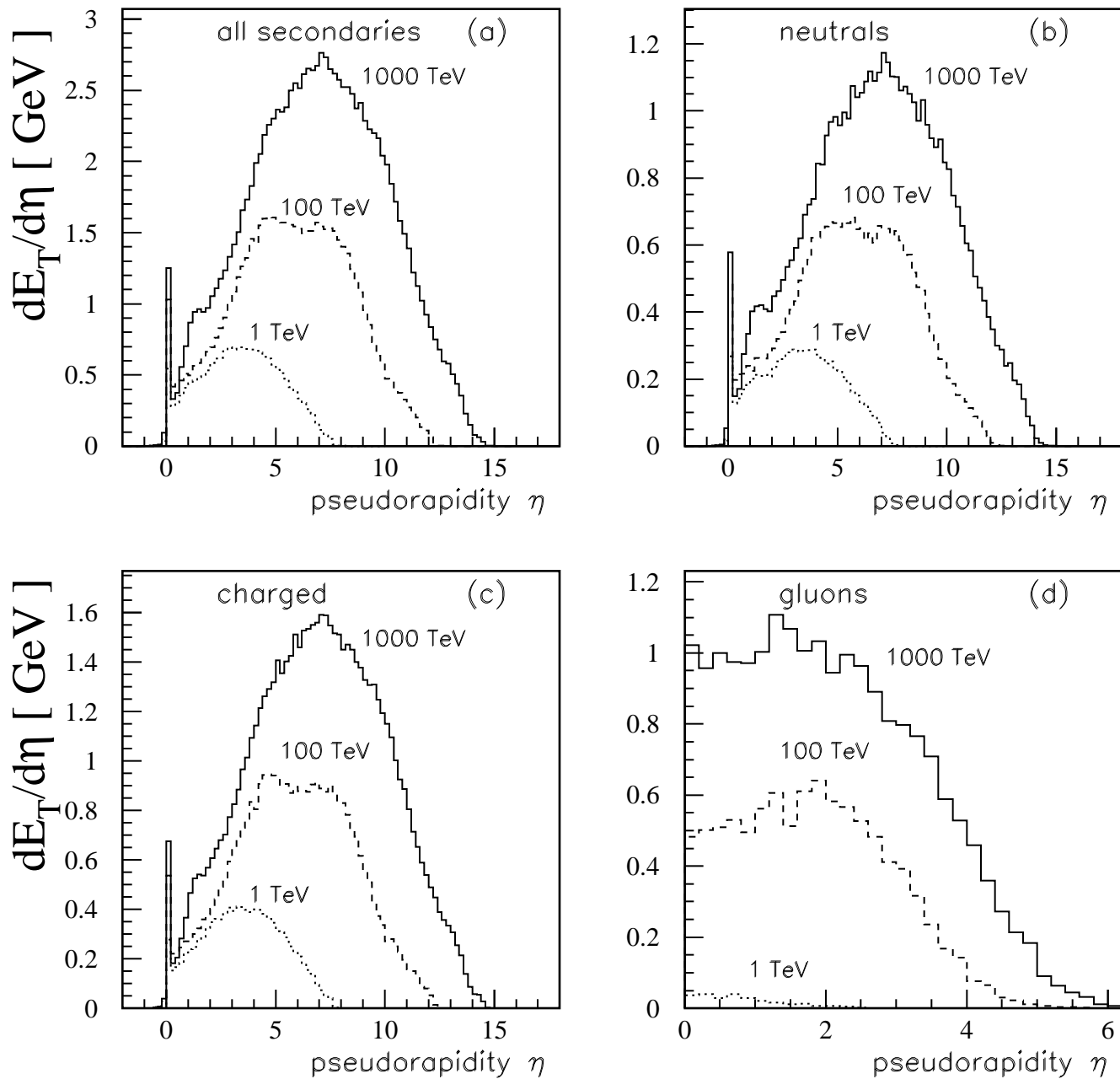


Figure 5

p+Air 1 TeV–1000 TeV 10^4 events ($b=0-5$ fm) HIJING

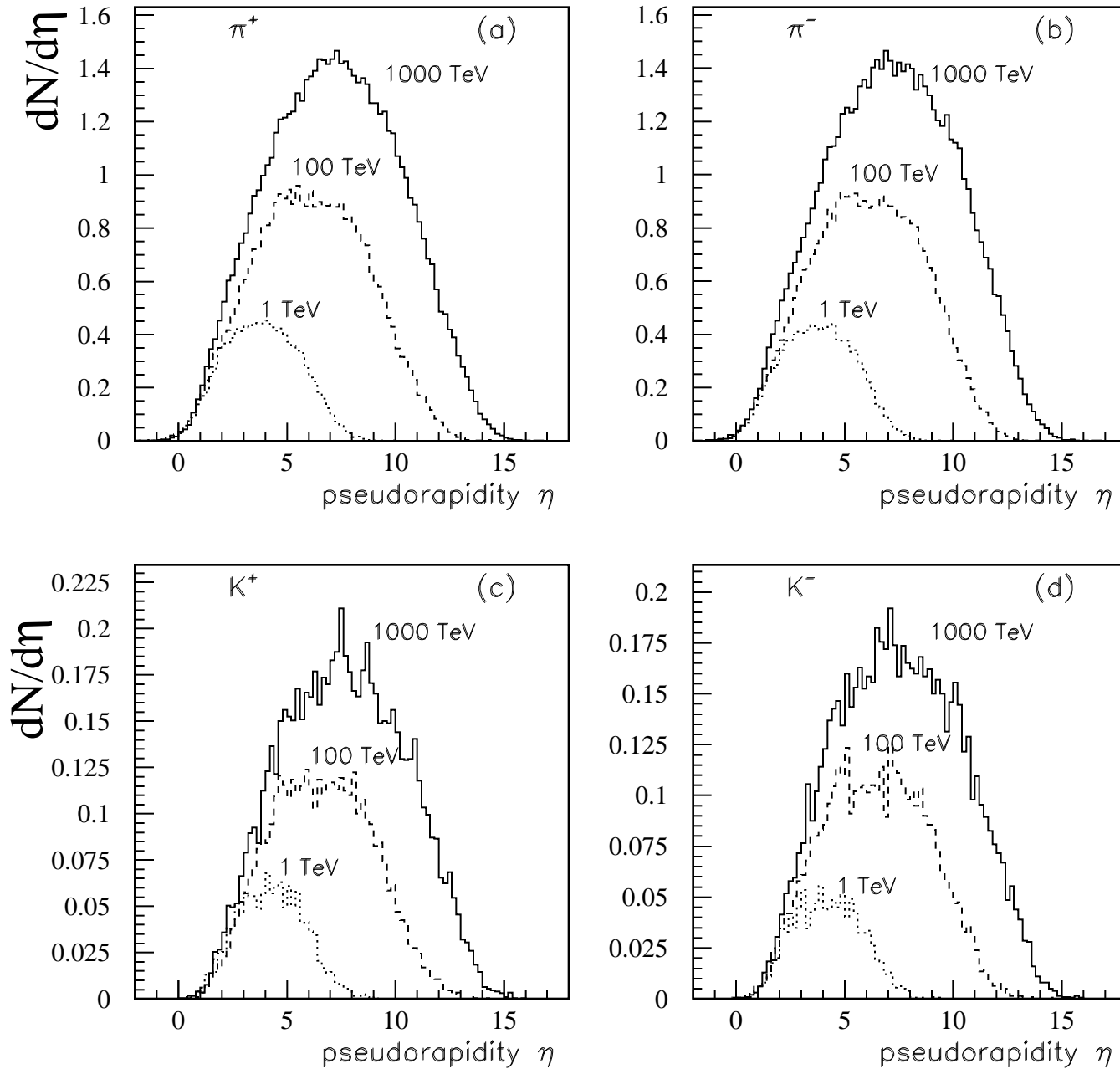


Figure 6

p+Air 1 TeV–1000 TeV 10^4 events ($b=0-5$ fm) HIJING

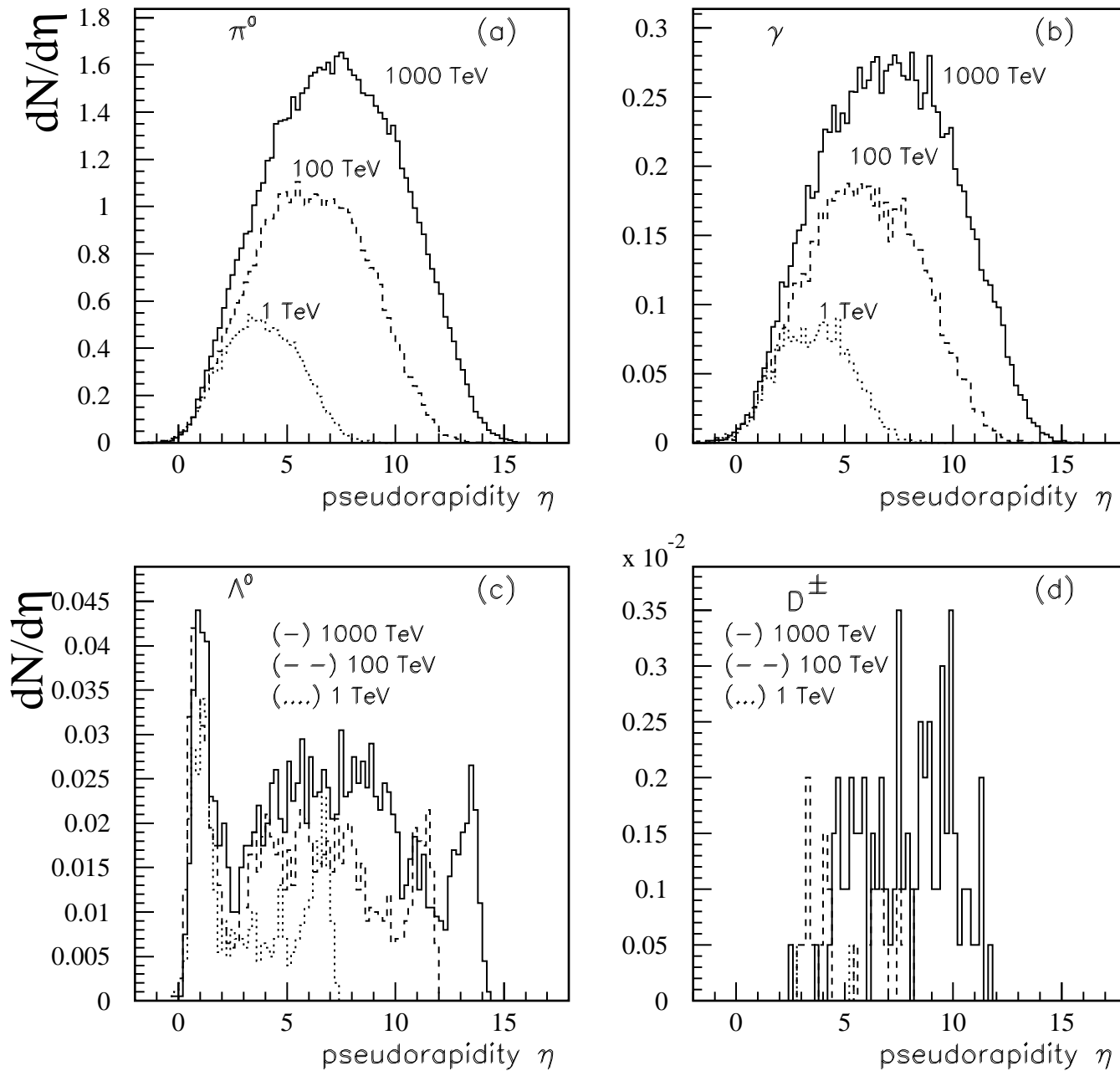


Figure 7

p+Air 1 TeV–1000 TeV 10^4 events ($b=0-5$ fm) HIJING

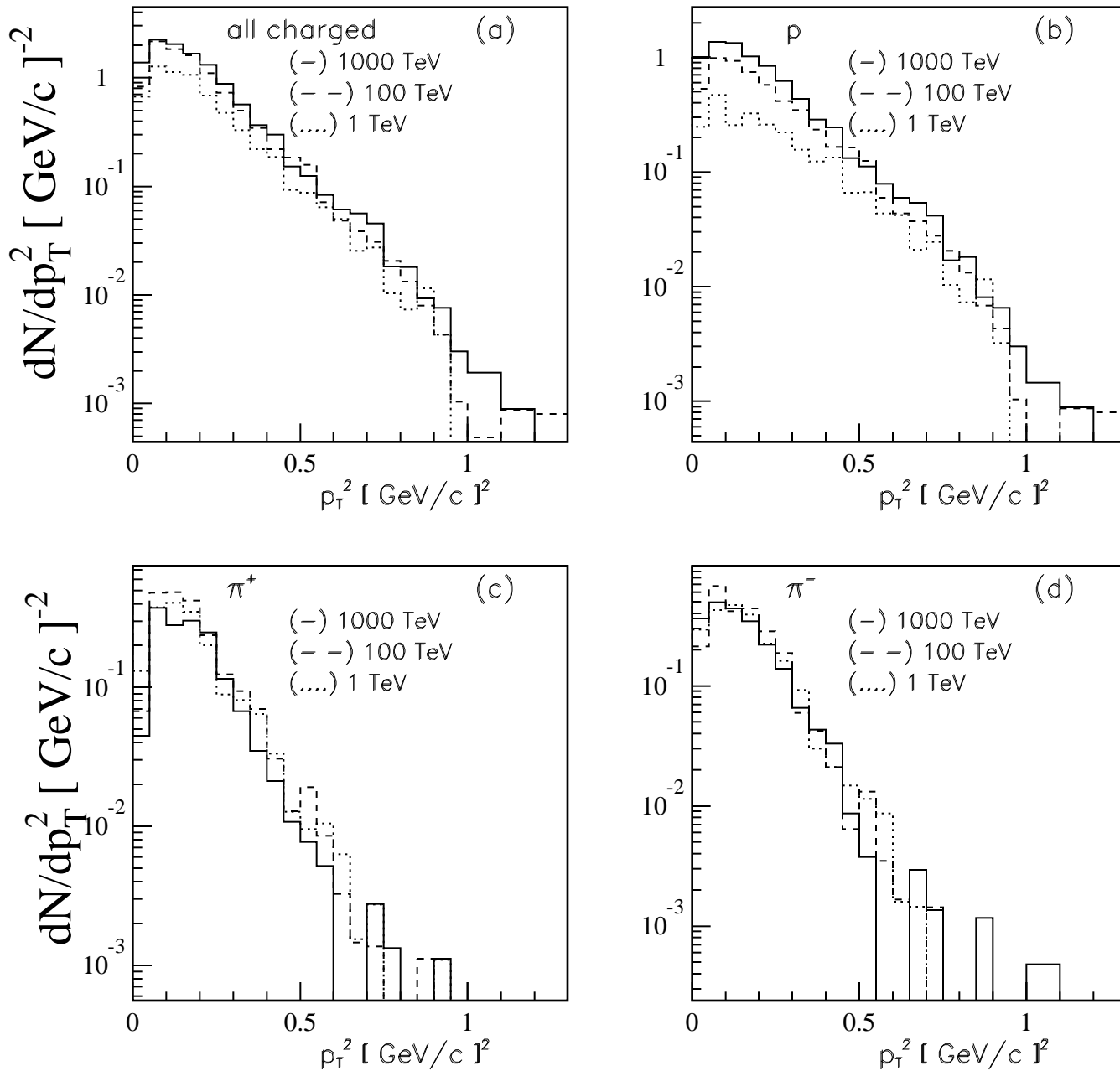


Figure 8

p+Air 1 TeV–1000 TeV 10^4 events ($b=0-5$ fm) HIJING

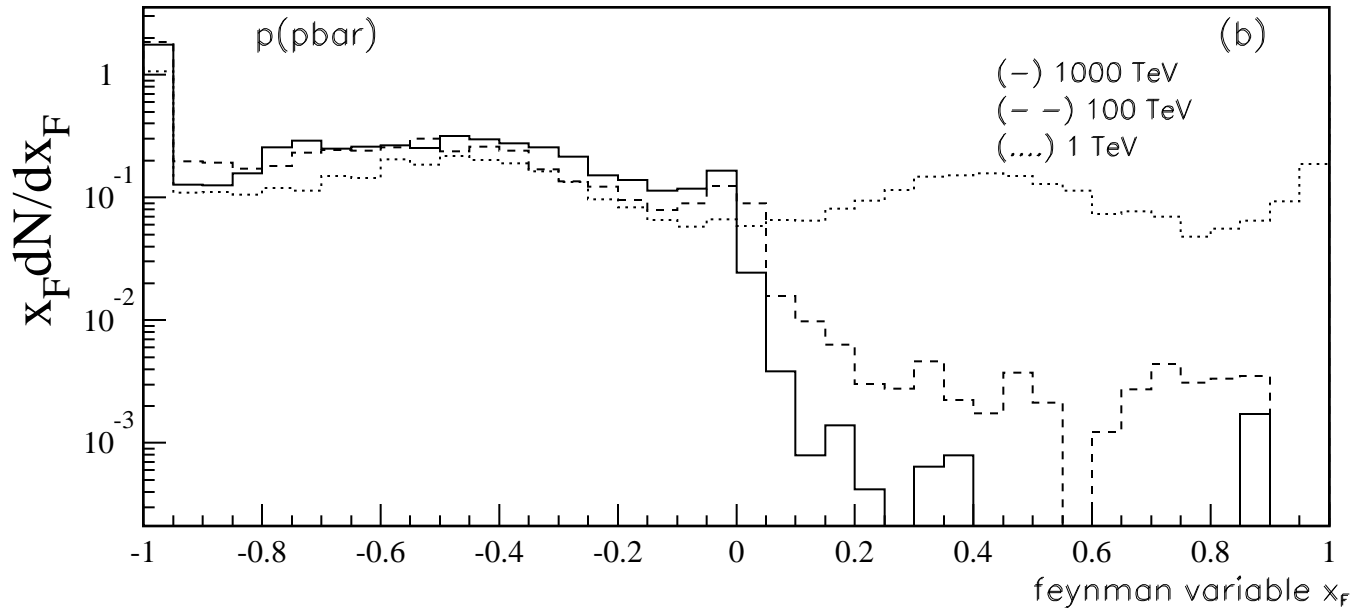
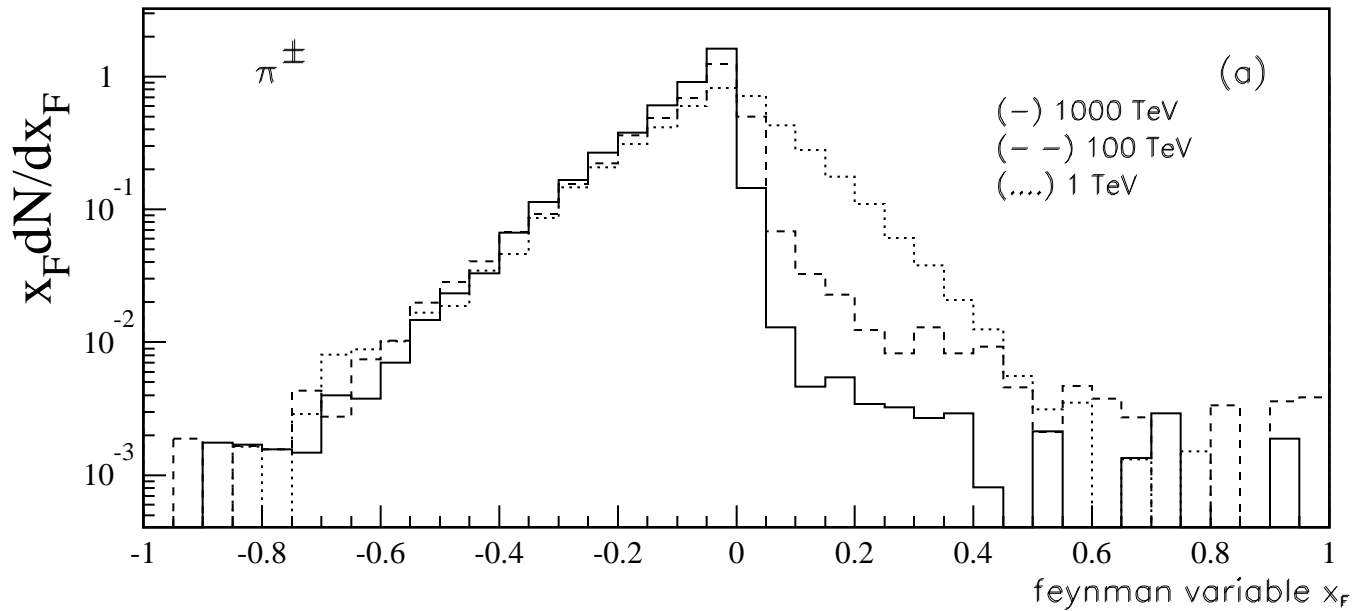


Figure 9

p+Air 1000 TeV 10^4 events ($b=0-5$ fm) HIJING

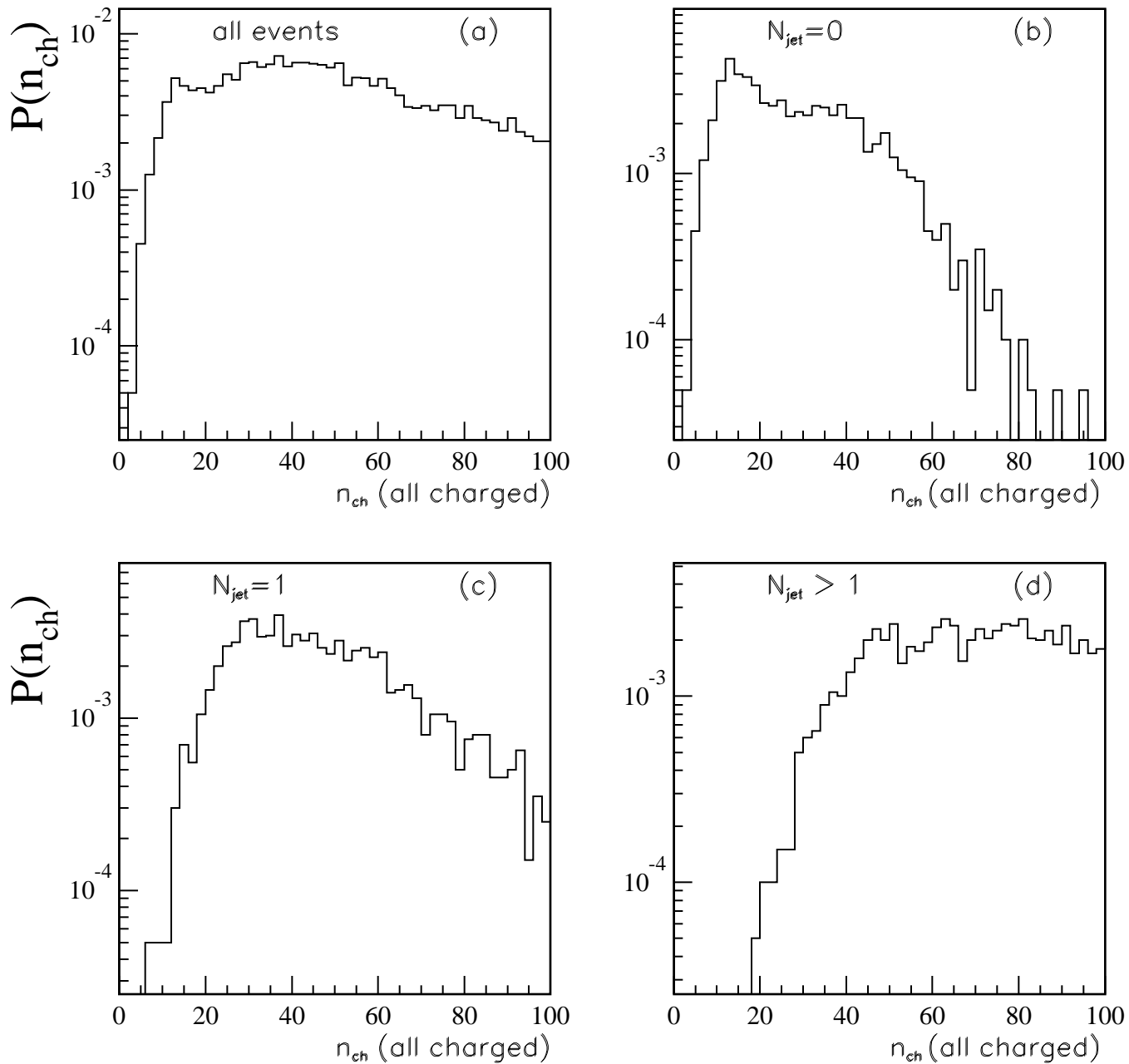


Figure 10

A+Air 17.86 TeV/Nucleon 10^4 events HIJING

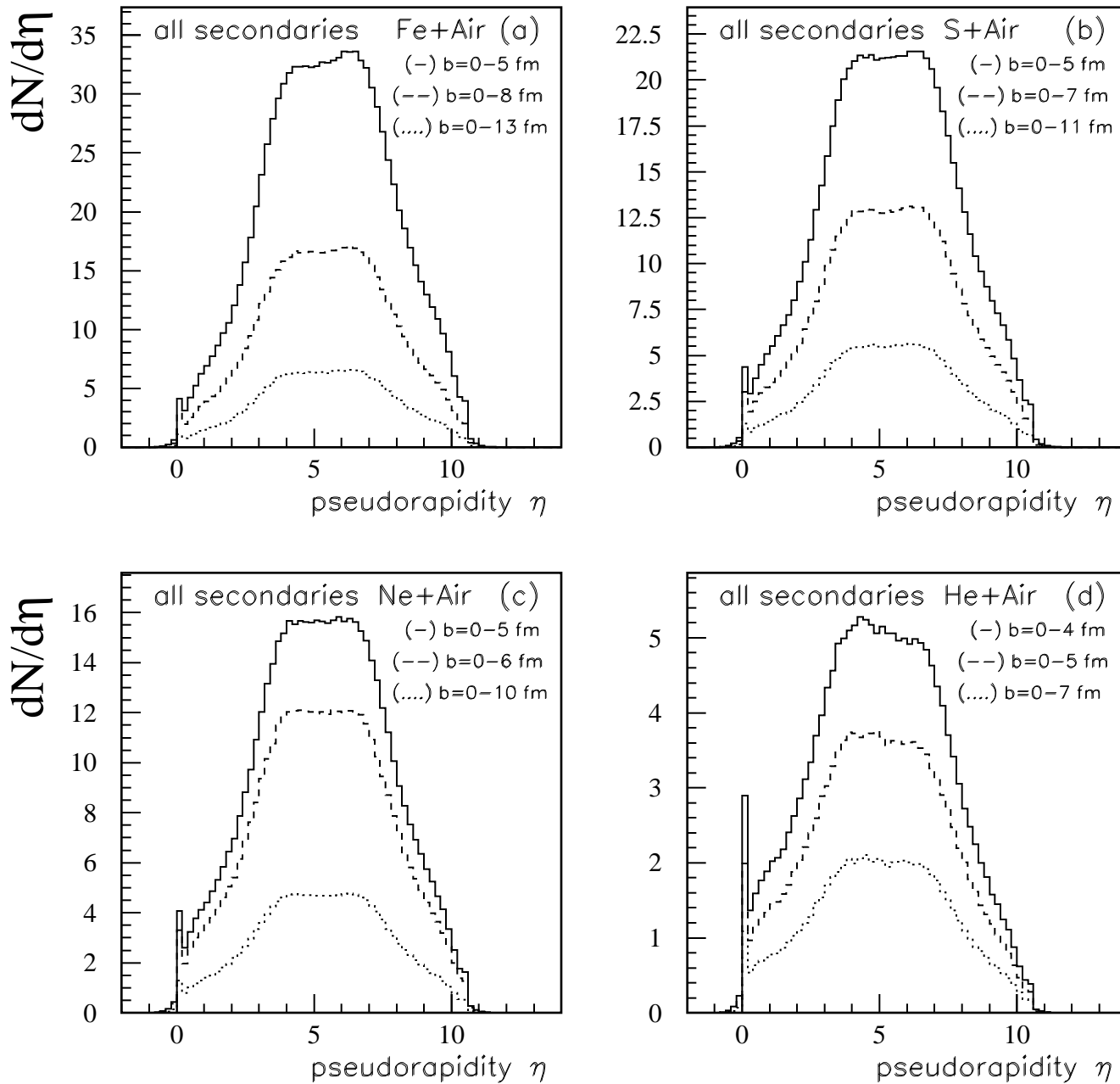


Figure 11

A+Air 17.86 TeV/Nucleon 10^4 events HIJING

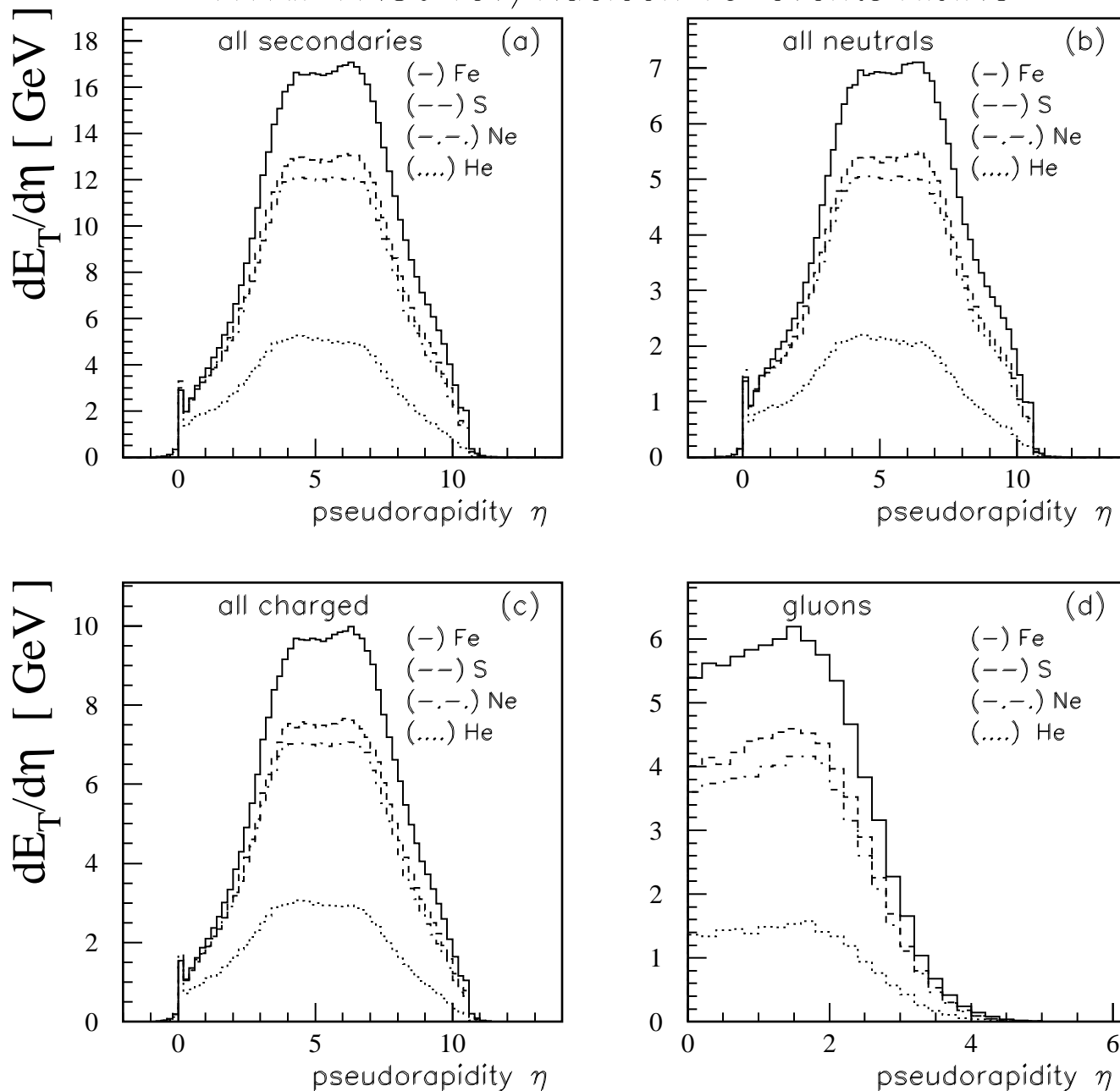


Figure 12

A+Air 17.86 TeV/Nucleon 10^4 events HIJING

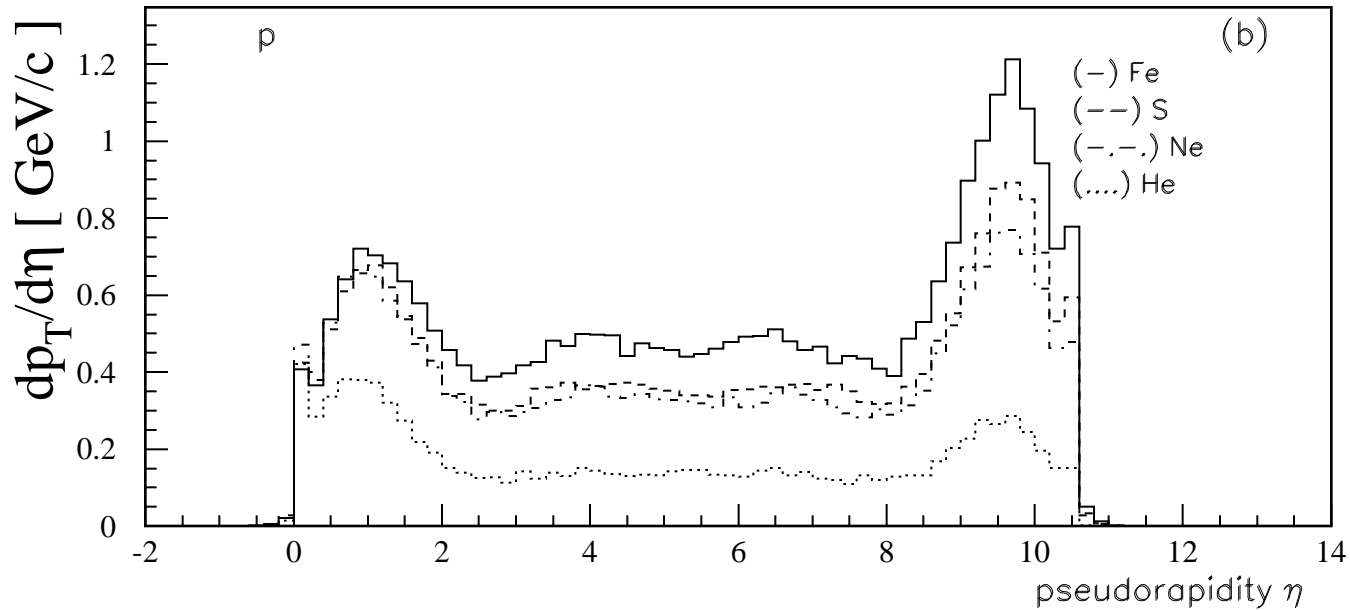
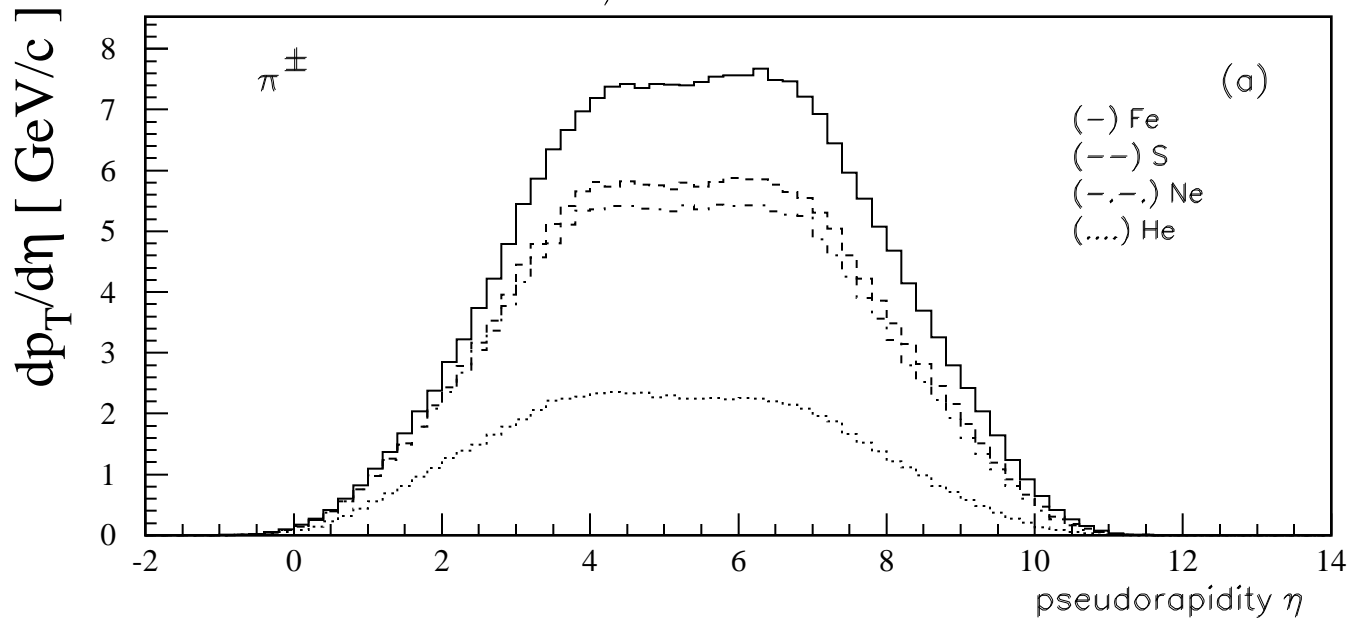


Figure 13

A+Air 17.86 TeV/Nucleon 10^4 events HIJING

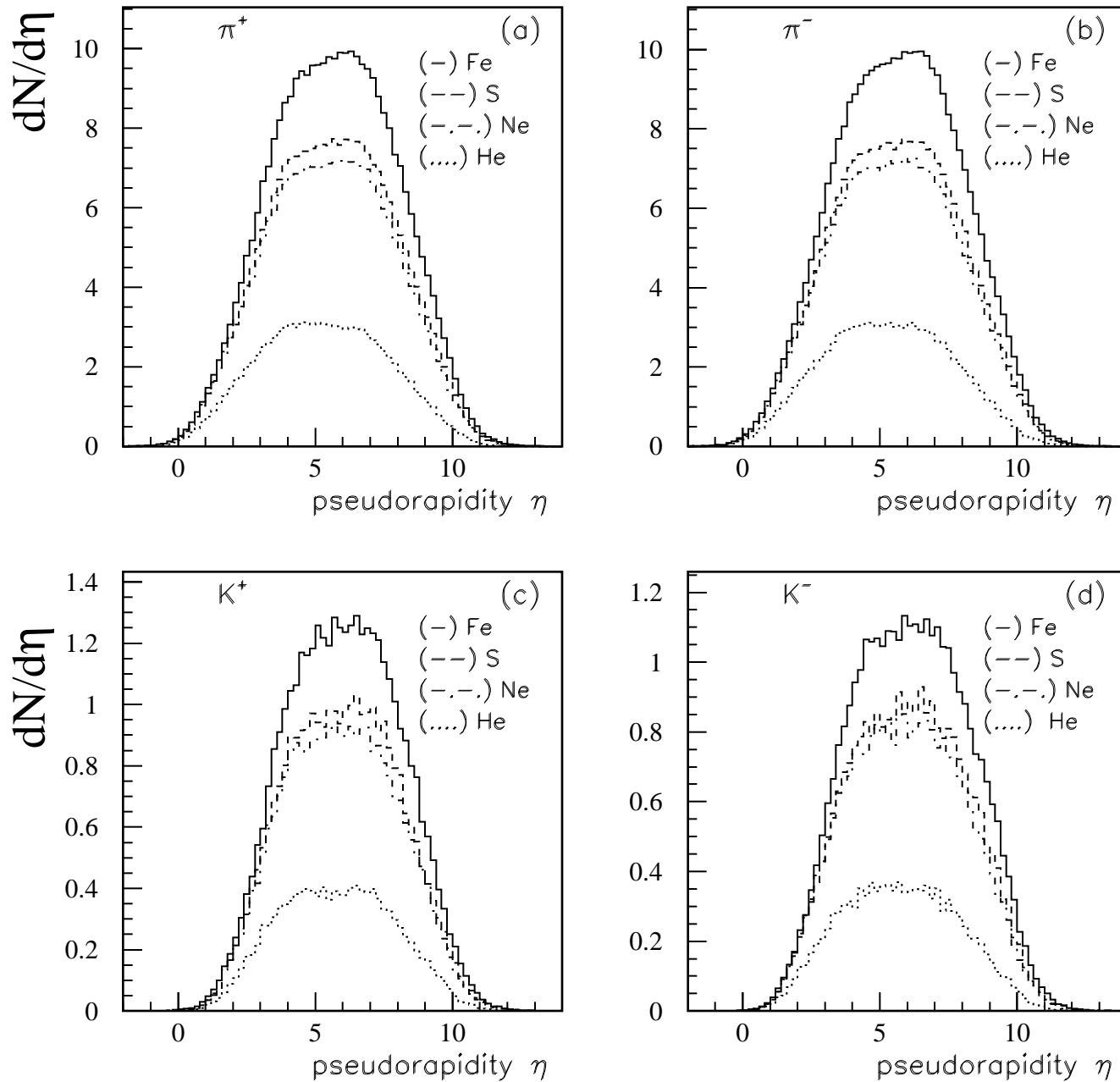


Figure 14

A+Air 17.86 TeV/Nucleon 10^4 events HIJING

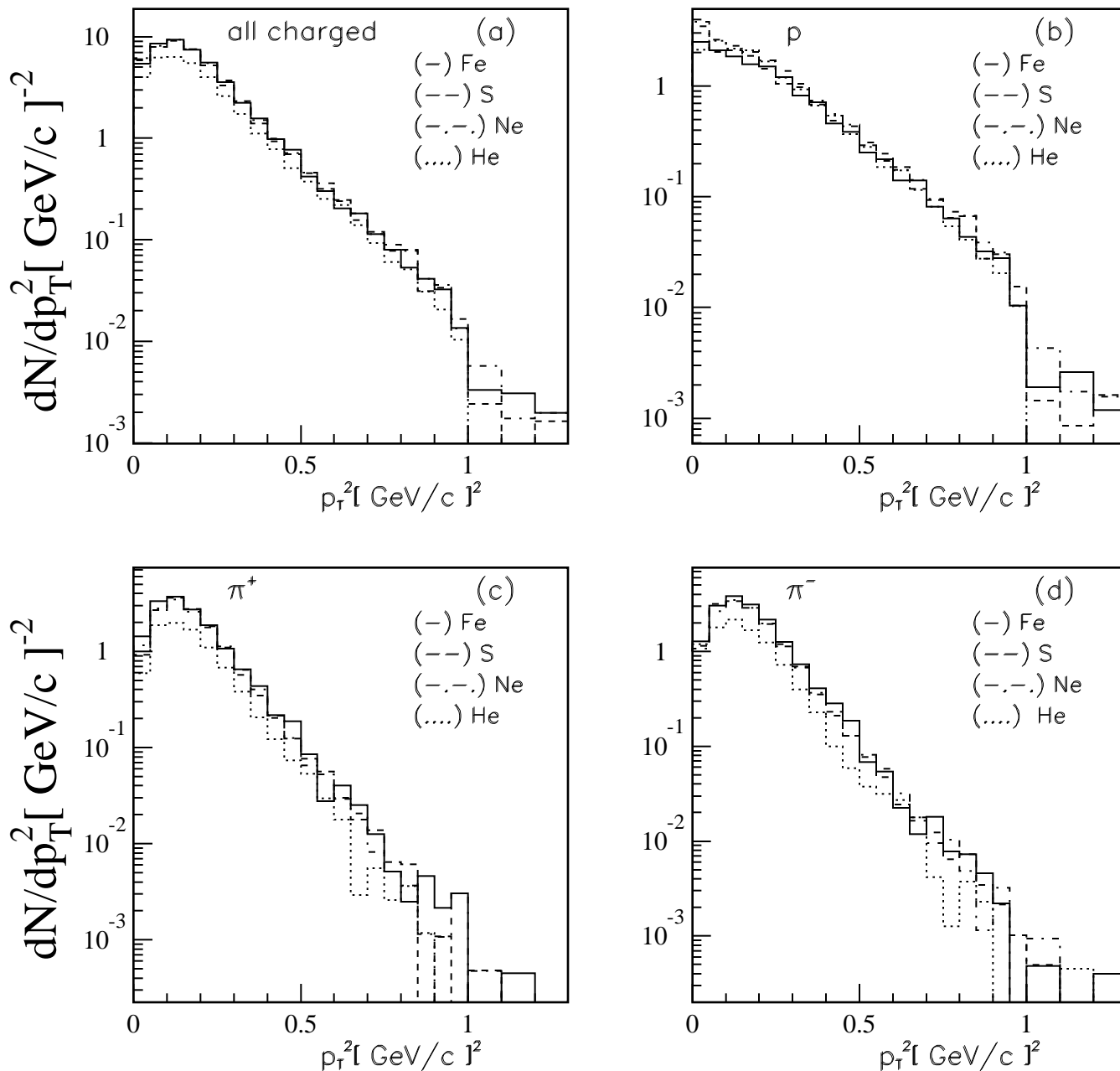


Figure 15

A+Air 17.86 TeV/Nucleon 10^4 events HIJING

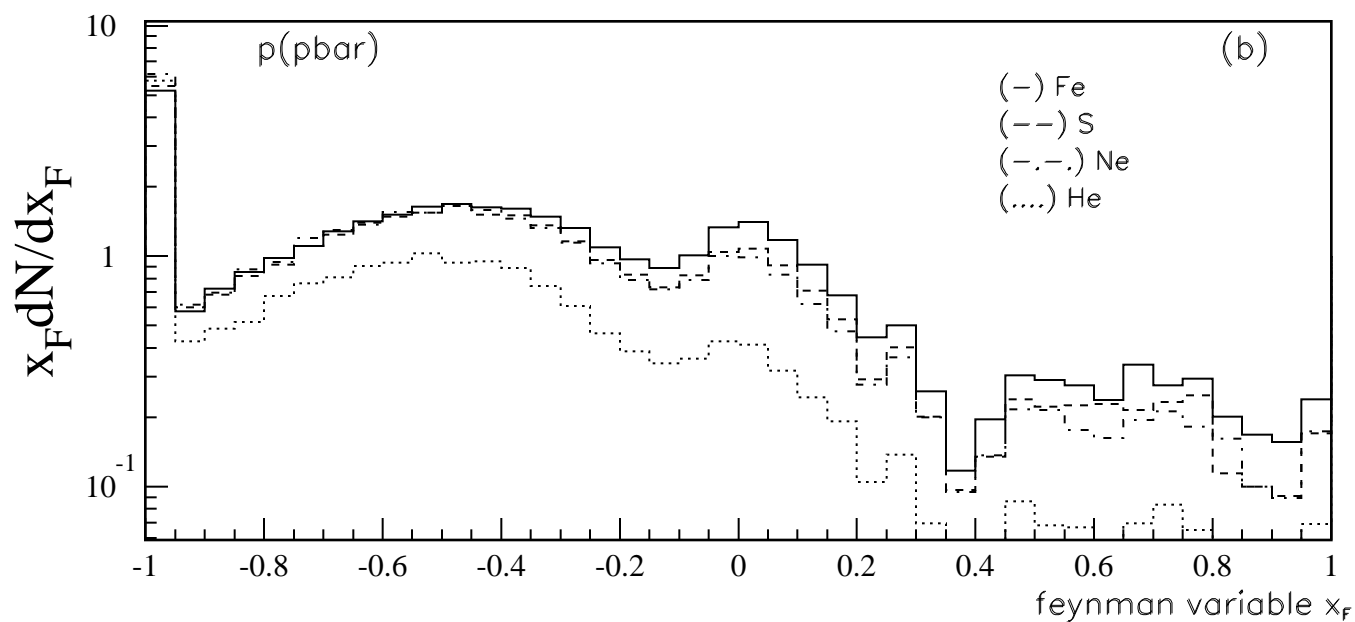
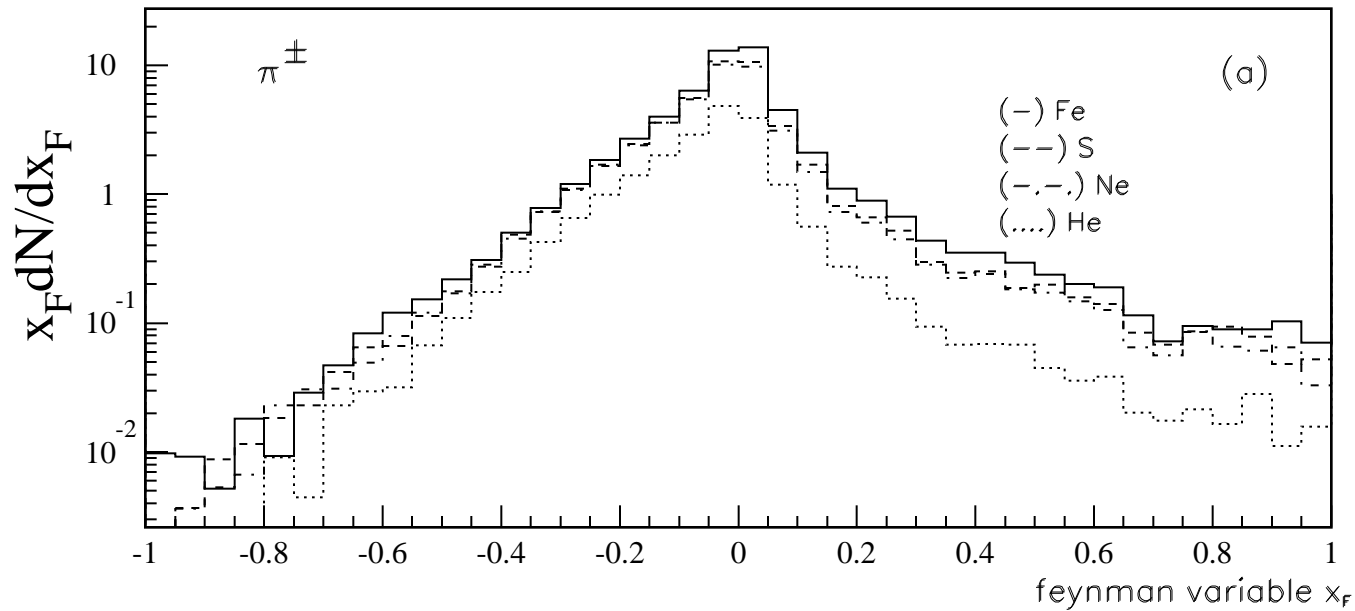


Figure 16

A+Air 17.86 TeV/Nucleon 10^4 events HIJING

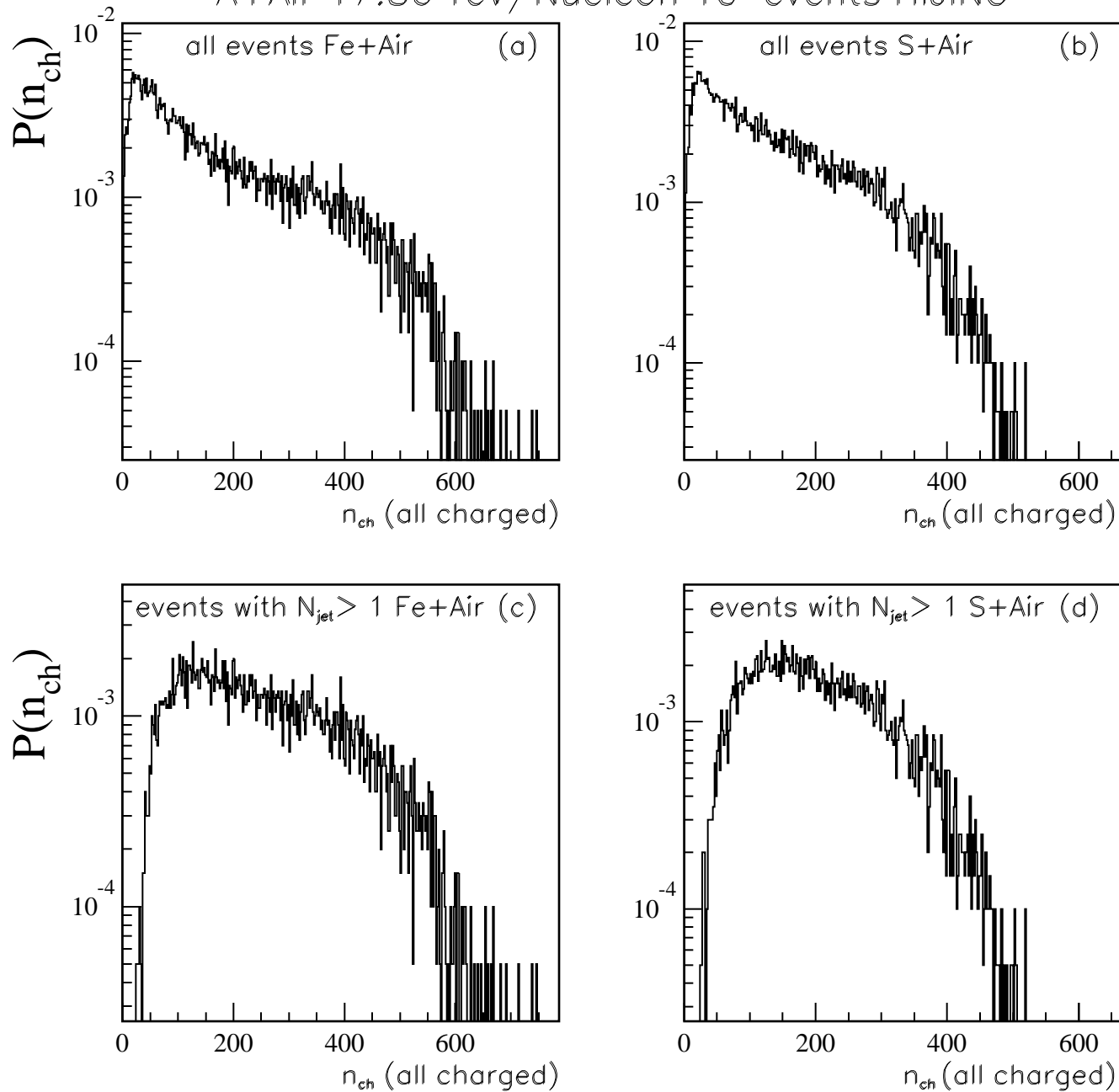


Figure 17

Fe+Air 17.86 TeV/Nucleon 10^4 events HIJING

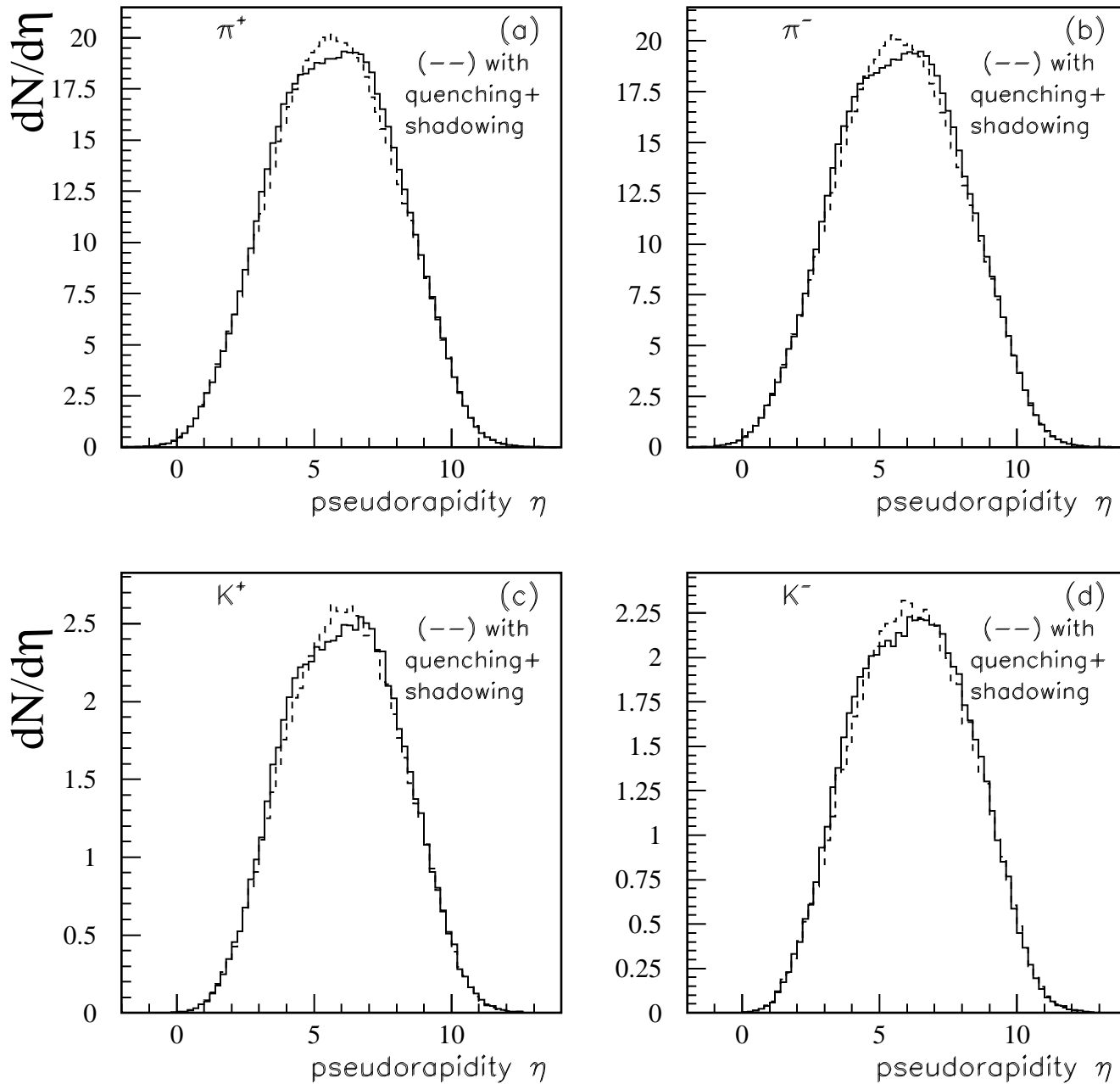


Figure 18

Fe+Air 17.86 TeV/Nucleon 10^4 events HIJING

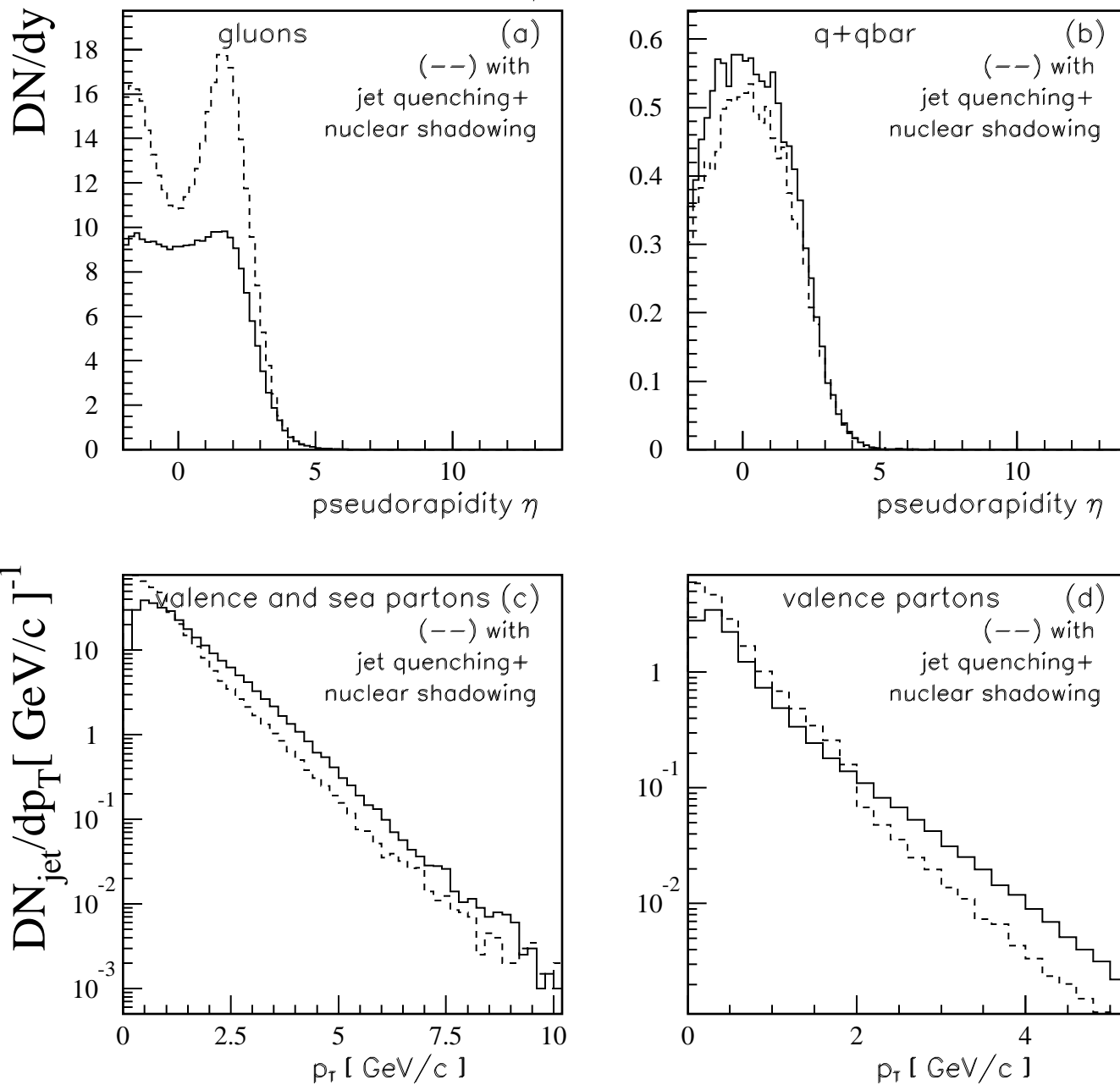


Figure 19